



HAL
open science

Electrospun Cactus Mucilage/Poly(vinyl alcohol) Nanofibers as a Novel Wall Material for Dill Seed Essential Oil (*Anethum graveolens* L.) Encapsulation: Release and Antibacterial Activities

Faten Mannai, Hanedi Elhleli, Anouar Feriani, Issei Otsuka, Mohamed Naceur Belgacem, Younes Moussaoui

► To cite this version:

Faten Mannai, Hanedi Elhleli, Anouar Feriani, Issei Otsuka, Mohamed Naceur Belgacem, et al.. Electrospun Cactus Mucilage/Poly(vinyl alcohol) Nanofibers as a Novel Wall Material for Dill Seed Essential Oil (*Anethum graveolens* L.) Encapsulation: Release and Antibacterial Activities. *ACS Applied Materials & Interfaces*, 2023, 15 (50), pp.58815-58827. 10.1021/acsami.3c13289 . hal-04388898

HAL Id: hal-04388898

<https://cnrs.hal.science/hal-04388898v1>

Submitted on 2 Nov 2024

HAL is a multi-disciplinary open access archive for the deposit and dissemination of scientific research documents, whether they are published or not. The documents may come from teaching and research institutions in France or abroad, or from public or private research centers.

L'archive ouverte pluridisciplinaire **HAL**, est destinée au dépôt et à la diffusion de documents scientifiques de niveau recherche, publiés ou non, émanant des établissements d'enseignement et de recherche français ou étrangers, des laboratoires publics ou privés.

This document is confidential and is proprietary to the American Chemical Society and its authors. Do not copy or disclose without written permission. If you have received this item in error, notify the sender and delete all copies.

Electrospun cactus mucilage/polyvinyl alcohol nanofibers as novel wall material for dill seed essential oil (*Anethum graveolens* L.) encapsulation: release and antibacterial activities

Journal:	<i>ACS Applied Materials & Interfaces</i>
Manuscript ID	Draft
Manuscript Type:	Article
Date Submitted by the Author:	n/a
Complete List of Authors:	Mannai, Faten; University of Gafsa, Faculty of Sciences of Gafsa Elhleli, Hanedi; University of Gafsa, Faculty of Sciences of Gafsa Feriani, Anouar; University of Gafsa, Faculty of Sciences of Gafsa Otsuka, Issei; Centre de Recherches sur les Macromolecules Vegetales, Belgacem, Mohamed Naceur; Universite Grenoble Alpes, Moussaoui, Younes; University of Gafsa Faculty of Sciences of Gafsa,

SCHOLARONE™
Manuscripts

1
2
3
4
5
6
7 Electrospun cactus mucilage/polyvinyl alcohol
8
9
10
11 nanofibers as novel wall material for dill seed
12
13
14
15 essential oil (*Anethum graveolens* L.) encapsulation:
16
17
18
19 release and antibacterial activities
20
21
22
23

24 *Faten Mannai, Hanedi Elhleli, Anouar Feriani, Issei Otsuka, Mohamed Naceur Belgacem,*
25
26 *Younes Moussaoui*
27
28
29
30
31
32
33

34
35 **KEYWORDS:** Polyvinyl alcohol, cactus mucilage, dill seed essential oil, emulsion
36
37
38 electrospinning, nanofibers, antibacterial.
39
40
41
42
43
44
45

46 **ABSTRACT:** The goal of this work was to make a long-lasting carrier by making dill seed
47
48
49 (*Anethum graveolens* L.) essential oil-loaded electrospun nanofibers from cactus mucilage (CM)
50
51
52
53 and polyvinyl alcohol (PVA). Continuous and homogeneous nanofibers with an average
54
55
56
57
58
59
60

1
2
3 diameter ranging between 158 ± 18 and 230 ± 26 nm were successfully electrospun from the
4
5
6
7 CM/PVA blend solution and the CM/PVA/DSEO emulsion. Atomic force microscopy
8
9
10 topographic images revealed that the electrospun nanofibers had a tubular morphology. The
11
12
13 TGA curves of DSEO, CM, pure PVA, and electrospun nanofibers show successful chemical
14
15
16 interactions between the polymers used and the essential oil. The water contact angle results
17
18
19 suggest that the manufactured nanofibers are hydrophilic. CM/PVA consistently achieves a
20
21
22 remarkable encapsulation efficiency of 100% DSEO. The electrospun nanofibers allowed for
23
24
25 controlled release of free and encapsulated DSEO, with sustained long-term oil release. The agar
26
27
28 disk diffusion technique was used to study the antimicrobial activity of electrospun nanofibers
29
30
31 and nanofibers containing DSEO against Gram-positive and Gram-negative bacteria. Electrospun
32
33
34 nanofibers containing DSEO exhibited bacteriostatic and bactericidal activities against
35
36
37 foodborne pathogenic bacteria (*S. aureus* and *P. aeruginosa*) with MICs of 2.5 mg/mL and MBCs
38
39
40 of 5 mg/mL. The electrospun nanofibers based on carbohydrates loaded with DSEO demonstrate
41
42
43 potential as an active internal coating for food packaging and biomedical applications.
44
45
46
47
48
49
50
51
52
53
54
55
56
57
58
59
60

1. INTRODUCTION

Electrospinning is one of the progressing technologies in nanofiber production. It is a versatile and potentially useful technique for creating micro- and nanoscale fiber mats with effective morphological and mechanical properties.¹ Electrospinning is a current and simple technique that uses high electric fields to stretch polymer solutions or melts to produce long-lasting and continuous fibers with 10–1000 nm diameters.^{2,3} Solution electrospinning is more commonly employed for the production of nanofibers than melt electrospinning. It is mainly used because of its low cost and potential for use in laboratory research and nanofibers' industrial production.⁴ For solution electrospinning, various kinds of organic polymers dissolved in solution form are adopted to produce nanofibers and nonwovens. Electrospinning has different factors that affect polymer solutions, such as polymer molecular weight, viscosity, concentration, solvent volatility, conductivity, and surface tension, and the electrospinning process, such as spinning voltage, spinning flow rate, needle tip to collector distance, temperature, and humidity.⁵ Electrospun nanofibers can be produced based on synthetic organic polymers and blends of solutions with natural polymers, including proteins, nucleic acids, and polysaccharides.^{6,7} The use of biopolymers in electrospinning has attracted great attention due to their large specific surface

1
2
3 area, good biocompatibility, biological activity, biodegradability, and non-toxicity, as well as
4
5
6 their diversified potential in technical and biomedical applications such as functional textiles,
7
8
9
10 filtration membranes, tissue engineering scaffolds, wound healing, drug delivery, cosmetics,
11
12
13 essential oil encapsulation, and active packaging.^{6,8-11} Despite recent progress in the
14
15
16 conventional electrospinning process, technological challenges exist to produce core-shell
17
18
19 nanofibers using emulsion electrospinning. It is a novel and simple method that has rapidly
20
21
22 developed and has received increasing interest as the process is considered more stable for
23
24
25 encapsulating therapeutic and bioactive compounds and essential oils within a single carrier.¹² In
26
27
28 the electrospinning process, selecting a suitable encapsulation material is important and is widely
29
30
31 studied depending on the nature of the uses for food, biomedicine, and other applications. In this
32
33
34 way, materials from renewable and alternative resources are used as appropriate wall materials
35
36
37 for emulsion electrospinning, such as biopolymers like proteins and polysaccharides, including
38
39
40 mucilage, cellulose and derivatives, starch, chitosan, etc., and biocompatible polymers essentially
41
42
43 the polyvinyl alcohol, polyethylene oxide, and polycaprolactone.¹²⁻¹⁷ Polyvinyl alcohol is a non-
44
45
46 ionic hydrolysis derivative of polyvinyl acetate. It is a highly hydrophilic semi-crystalline
47
48
49
50
51 polymer with excellent mechanical properties.¹⁸ PVA is commonly used alone or blended with
52
53
54
55
56
57
58
59
60

1
2
3 natural polymers to produce electrospun nanofibers. The emulsion-based electrospun nanofibers
4
5
6
7 are made from blended polymers according to their type and specific uses.¹⁹ Moreover, the
8
9
10 emulsion electrospinning process is proposed as an effective way to encapsulate the essential oil
11
12
13 in fiber-forming materials. The encapsulation efficiency tends to be 100%. Electrospun
14
15
16
17 nanofibers have proven their suitability as materials for the controlled release of essential oils.²⁰
18
19
20 This method is based on the electrospinning of stable biopolymeric emulsions, which can be
21
22
23 made by stabilizing water-in-oil or oil-in-water emulsions with an emulsifier or surfactant. These
24
25
26
27 emulsions can then be electrospun as spinning solutions. Meanwhile, other essential oils have
28
29
30 been loaded into electrospun fibers, like thyme essential oil,²¹ costmary essential oil,²² cinnamon
31
32
33 essential oil,²³ orange essential oil,²⁰ cabreuva essential oil¹⁵ and cumin essential oil.²⁴ In this
34
35
36
37 case, DSEO was microencapsulated through emulsion electrospinning, and, for this reason, CM
38
39
40 is a fascinating and interesting core-shell material for emulsion electrospinning. Additionally,
41
42
43
44 PVA can be blended with mucilage and used as a fibrous carrier for essential oils. The oil-in-
45
46
47 water emulsion was prepared using a high-speed homogenization process.

50
51 Essential oils have been widely exploited for their biological properties, mainly as
52
53
54 antimicrobials in the food, pharmaceutical, and biomedical fields. Encapsulation of essential oils
55
56
57
58
59
60

1
2
3
4 is necessary to protect their functional properties because they have the characteristics of fast
5
6
7 release and a short duration of action. Emulsion electrospinning is a promising technique for
8
9
10 essential oil encapsulation to improve its sustained-release performance.²⁵ Essential oils from dill
11
12
13 seeds are the most valuable medicinal seed spice crops of the Apiaceae.²⁶ It is one such annual
14
15
16 aromatic herb, belonging to the family Umbelliferae.²⁷ DSEO is a potential inhibitor of bacterial
17
18
19 and fungal.²⁷⁻²⁹ Further, it was found that the essential oils of *Anethum graveolens* L. seeds have
20
21
22 been reported as a potential natural preservative in fish food due to their antioxidant and
23
24
25 antimicrobial activities.²⁸
26
27
28
29

30 The cactus, *Opuntia ficus-indica*, is a tree-like shrub that belongs to the *Cactaceae* family. It
31
32
33 is a suitable carbohydrate source and can adapt to various environmental conditions.³⁰ The cactus
34
35
36 biomass has been mainly used as a raw material for added-value materials with different
37
38
39 applications, such as reinforcing agents for the production of composite materials,^{31,32}
40
41
42 papermaking^{33,34} and wastewater treatment.³⁵ The cactus mucilage extracted from the cladode is
43
44
45 a heteropolysaccharide of an anionic polyelectrolyte nature with a high molecular mass, mainly
46
47
48 composed of L-arabinose, D-galactose, D-xylose, L-rhamnose, and α -D-(1 \rightarrow 4) galacturonic
49
50
51 acid.³⁶ CM exhibits an effective functional property due to the hydrogen bonding between
52
53
54
55
56
57
58
59
60

1
2
3 different functional and other polar groups. Cactus mucilage has been utilized in food as a
4
5
6
7 thickener, in cosmetics, and in pharmaceuticals as a wall material for encapsulation
8
9
10 processes³⁷⁻³⁹ as well as in film-forming.⁴⁰
11
12

13
14 To the best of our knowledge, there have been no previous reports of DESO loading into
15
16
17 blended CM and PVA electrospun nanofibers. The DSEO was extracted from ground dill seeds
18
19
20 using hydrodistillation, and the oil's chemical composition was identified using gas
21
22
23 chromatography coupled to mass spectrometry. The CM was extracted with hot water and a
24
25
26 sonication process from fresh cladodes and then precipitated with ethanol. The CM extracted
27
28
29 using ethanol as the extraction solvent is considered non-toxic and safe for human and animal
30
31
32 consumption. The spinning solution and emulsion were created by combining CM and PVA. The
33
34
35 oil-in-water emulsion was carried out using DSEO as the oily phase and a CM/PVA blend
36
37
38 solution as the aqueous phase. The pH, viscosity, conductivity, and surface tension of the
39
40
41 obtained solutions were controlled. The polymer solutions were used to formulate neat PVA/CM,
42
43
44 and loaded CM/PVA/DSEO electrospun nanofibers. They were considered an alternative to
45
46
47
48
49
50 producing nanostructures and encapsulating the essential oil during fiber formation by the
51
52
53
54
55
56
57
58
59
60

1
2
3 electrospinning method. The electrospun fiber morphology, structural and thermal properties,
4
5
6
7 and water contact angles were determined. The DSEO release was controlled.
8
9

10 11 **2. EXPERIMENTAL SECTION** 12 13

14 15 **2.1. Extraction and characterization of essential oil from dill seeds.** 16 17

18
19 Dill seed was collected from the El-Guettar oasis, near Gafsa, in the south-west of Tunisia. The
20
21
22 extraction of the dill seed essential oil was carried out by the hydrodistillation method.
23
24
25
26 Approximately 100 g of the powdered dill seeds ($\geq 45 \mu\text{m}$) were immersed in 2 L of distilled
27
28
29 water, and the resulting mixture was hydrodistilled for 3 h (until there was no more water to
30
31
32 evaporate). The DSEO were separated, dried with anhydrous sodium sulfate, and stored in a dark
33
34
35
36 glass vial at 4 °C for further experiments. The chemical characterization of DSEO was carried
37
38
39 out by gas chromatography/mass spectrometry (GC/MS, GC 7890A, MS 5975C, Agilent, Santa
40
41
42 Clara, CA, USA). About 0.01 g of dill seed essential oil was dissolved in 1 ml of ethyl acetate,
43
44
45
46 and then this solution was injected into a capillary column (Agilent, 0.25 mm \times 30 m). The
47
48
49 conditions used to perform the GC/MS analysis were as follows: the injector was at 280 °C with
50
51
52 the split/splitless method in split mode (10:1); the carrier gas washes helium with a flow rate of
53
54
55
56 0.7 mL/min; the temperature ramp started at 50 °C and was increased by 10 °C/min to 120 °C
57
58
59
60

1
2
3 and maintained for 5 min; in the second stage of the ramp, the temperature was increased from
4
5
6
7 10 °C/min to 280 °C and maintained for 8 min; finally, in the third stage, the temperature was
8
9
10 increased by 10 °C/min to 300 °C and kept constant for 2 min. The identification of all
11
12
13 components was studied using a relative peak area percentage. An attempt to identify the
14
15
16
17 compounds was made based on the comparison of their relative retention times and mass spectra.
18
19
20 The confirmation of the identified components of the dill seed essential oil was carried out with
21
22
23 the National Institute of Standards and Technology (NIST). Essential oil components were
24
25
26
27 determined using the NIST library.
28
29
30

31 **2.2. Extraction of cactus mucilage**

32
33
34 CM was extracted from fresh cladodes harvested from the El-Guettar oasis, near Gafsa in the
35
36
37 south-west of Tunisia, and cleaned and washed with distilled water. Fresh cladode pieces (1×1×1
38
39
40 cm³) were homogenized with distilled water (1:1 w/v), soaked overnight, and then boiled at 80
41
42
43 °C for 40 minutes under mechanical stirring. After cooling, the mixture was put in an ultrasonic
44
45
46 bath for 40 minutes at 40 °C. Thus, the mixture was filtered three times through a nylon filter to
47
48
49
50 separate the liquid from the solids and centrifuged for 20 minutes at 4000 rpm at 25 °C. The
51
52
53
54 liquid was recovered and precipitated with ethanol (96% purchased from Sigma-Aldrich) at a
55
56
57
58
59
60

1
2
3 ratio of 1:3 (v:v). Precipitation was performed at 4 °C overnight. The CM was washed with pure
4
5
6 ethanol (99% purchased from Sigma-Aldrich) and acetone (99% purchased from Sigma-
7
8
9 Aldrich), dried at 45 °C for 24 hours, and then stored in bottles and dark glass. The extraction
10
11
12
13 yield of CM was $22.8 \pm 2.4\%$.
14
15
16
17

18 **2.3. Preparation of spinning solution**

19
20

21 The CM solution was prepared by introducing 2 g of dried CM into 100 mL of distilled water.
22
23
24 The mixture was homogenized using magnetic stirring overnight at room temperature and
25
26
27 humidity. The concentration of PVA (Mw: 145000 g/mol, bought from Sigma-Aldrich) was set
28
29
30 at 15 wt%, and was dissolved at 70 °C for 3 hours with magnetic stirring to make a thick solution
31
32
33
34 that could be electrospun. After cooling, the CM/PVA mixture was prepared in a ratio of 80:20
35
36
37 (w/w) under magnetic stirring for 30 min. The oil-in-water emulsion was made with a dispersed
38
39
40
41 oil phase of 4% DSEO (w/w, oil/polymeric aqueous solution) and a continuous phase of
42
43
44 CM/PVA solution. The Tween 80 was used as an emulsifier (1.2 wt% of the oil mass). The
45
46
47 mixture was then vigorously dispersed with an ultraturrax high-speed homogenizer (Ika T 25
48
49
50 basic, France) at room temperature (≈ 20 °C) and 11000 rpm for 15 min to better stabilize the oil
51
52
53
54 droplets in the CM/PVA solution.
55
56
57
58
59
60

2.4. Electrospinning

The electrospinning of CM/PVA and CM/PVA/DSEO mixtures was performed using Esprayer ES-2000S2A equipment (Fuence Co., Ltd., Tokyo, Japan) at 25°C and a relative humidity of 34%. A metallic electrode plate wrapped with aluminum foil was placed 15 cm (depending on the sample) away from the needle (Nordson Stainless Steel Tips, 18 Gauge; inner diameter = 0.84 mm; outer diameter = 1.27 mm). High voltage (30 kV) was applied between the needle and the electrode plate while the mucilage-blend solution flowed with a latency of 20 μ L/min from the needle to collect the electrospun product on the aluminum foil. The electrospun products on the aluminum foils were dried at room temperature in desiccators. [Figure 1](#) shows the scheme for the preparation of electrospun nanofibers.

2.5. Characterization of solutions

The conductivity and pH of the different samples were measured using a Seven Easy™ S30 conductivity meter, Belgium, and a Proviteq pH meter, France, respectively. The viscosity of the different solutions and emulsions was measured at 20 °C using a rotational rheometer with a 50-mm cone-plane measurement system (Anton Paar, PHYSICA MCR302 viscometers). This

makes it possible to measure the variation of viscosity (η) as a function of time and the speed of shear ($\dot{\gamma}$) from 10^{-3} to 10^3 s $^{-1}$.

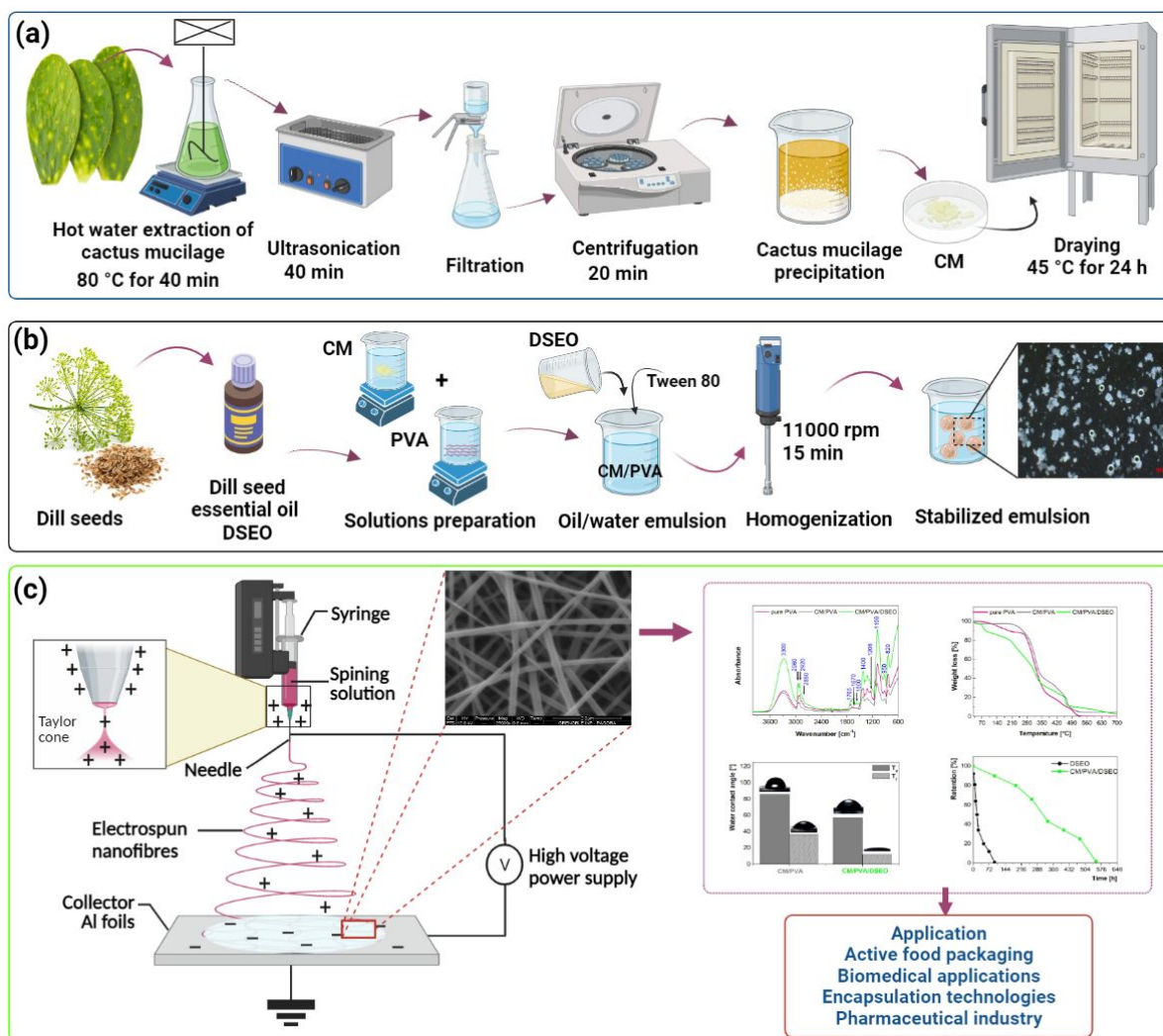


Figure 1. Schematic illustration of procedures used to produce electrospun nanofibers: (a) cactus mucilage extraction, (b) spinning solution and emulsion preparations and (c) electrospun nanofibres formulation.

2.6. Morphological analysis

The morphology of the prepared emulsion was observed by optical microscopy. The morphology of electrospun nanofibers was studied by scanning electron microscopes (SEM) and atomic force microscopy (AFM). An optical microscope, the Axio Imager M1 (Carl Zeiss, Munich, Germany), was operated in transmission mode, and the emulsion sample was observed at a diluted concentration. At least 10 images were taken. The electrospun nanofibers on the aluminum foil were coated with a ca. 4-nm-thick layer of gold/palladium (Au/Pd) before scanning electron microscopy observation. The scanning electron microscopy was performed using a Quanta 250 FEG (Thermo Fischer) device equipped with a CCD camera with a resolution of 16 bits, and the accelerator voltage was fixed at 10 kV. Five micrographs for each sample were captured at different positions. The topography of electrospun nanofibers was characterized using multimodal atomic force microscopy (DI, Veeco, Instrumentation Group, Plainview, NY, USA). Samples (0.2×0.2 cm²) were deposited on a mica plate disc and then analyzed, and representative micrographs have been recorded and selected for results and discussion.

2.7. Fourier transmission infrared analysis

1
2
3
4 The infrared spectra of samples were carried out on an Elmer Paragon 100 spectrometer using
5
6
7 an attenuated total reflectance (ATR) module composed of diamond crystals. The measurements
8
9
10 were recorded between 600 and 4000 cm^{-1} , with a resolution of 4 cm^{-1} and 20 scans.
11
12

13 14 15 **2.8. Thermal analysis** 16

17
18 The thermogravimetric analysis (TGA) of all samples was performed using an STA-6000
19
20 thermogravimetric analyzer (Perkin Elmer Instruments, Villebon-sur-Yvette, Grenoble, France).
21
22
23
24 Approximately 7 to 10 mg of sample were dynamically scanned between 30 and 700 °C at 10
25
26
27 °C/min under an oxygen stream with a flow rate of 20 mL min^{-1} .
28
29
30

31 32 33 **2.9. Contact angle** 34

35
36 Water contact angle measurement was performed with a Theta Flex optical tensiometer (Biolin
37
38 Scientific) using 5 μL water drops. The contact angles were recorded at initial drop contact on
39
40 the surface of the specimen (T_0) and after 20 s of drop contact on the surface (T_f). Three
41
42
43
44
45 measurements were performed for each sample at 20 °C.
46
47
48
49

50 51 52 **2.10. Encapsulation efficiency** 53 54 55 56 57 58 59 60

1
2
3 According to Yang et al.,⁴¹ the encapsulation efficiency (EE) of DSEO loaded into CM/PVA
4
5
6
7 nanofibers was studied by measuring the amount of oil located on the surface of electrospun
8
9
10 nanofibers (non-encapsulated oil). 60 mg of the electrospun fibers were put in hexane (7 mL) for
11
12
13 1 min with handshaking to remove the surface oil. The absorbance of the obtained liquid was
14
15
16
17 evaluated at a wavelength of 278 nm using a UV/vis spectrophotometer. The concentration of
18
19
20 dill seed essential oil in hexane was determined using a calibration curve ($R^2=0.99$) obtained by
21
22
23 dissolving different amounts of essential oil in hexane. The encapsulation efficiency was
24
25
26
27 calculated as follows:

$$EE = \frac{T - F}{T} \times 100$$

28
29
30
31
32
33
34
35 where, T was the total amount of dill seed essential oil, F was the free amount of dill seed
36
37
38 essential oil in the collection solution.⁴²
39
40
41
42

43 **2.11. Essential Oil release**

44
45
46 The release of free and encapsulated DSEO was controlled according to the method of Gómez-
47
48
49 Mascaraque et al.,⁴³ with some modifications. 2 mg of electrospun nanofibers were immersed in
50
51
52
53 7 mL ethanol and slowly stirred at room temperature. An aliquot of 1.5 mL solution was
54
55
56
57
58
59
60

1
2
3 removed and measured at a wavelength of 220 nm using a UV/vis spectrophotometer during
4
5
6
7 specific intervals of time. The same volume as that of the aliquot (1.5 mL) was replaced with
8
9
10 fresh ethanol at each interval.
11
12

13 14 **2.12. Antibacterial activity of electrospun nanofibers**

15 ***2.12.1. Bacterial strains and inoculums preparation***

16
17
18 To assess the potency of each sample's antibacterial properties, we tested them against five
19
20
21 bacterial strains that cause food poisoning. These strains included two types of Gram-positive
22
23
24 bacteria (*Staphylococcus aureus* and *Bacillus cereus*) and three types of Gram-negative bacteria
25
26
27 (*Escherichia coli*, *Salmonella typhi*, and *Pseudomonas aeruginosa*). The bacterial strains were
28
29
30 provided from the culture collection of the Department of Botany and Microbiology at the
31
32
33 Faculty of Sciences of Gafsa. Each bacterial strain was subcultured overnight at 35 °C on
34
35
36 Mueller-Hilton agar slants. Bacterial growth was harvested using 5 mL of sterile saline water; its
37
38
39 absorbance was adjusted to 580 nm and diluted to a viable cell count of 10⁷ CFU/mL using a
40
41
42 UV/vis spectrophotometer.
43
44
45
46
47
48
49
50

51 ***2.12.2. Antibacterial activity***

1
2
3 The disk diffusion method was used to evaluate the antimicrobial activity of the produced
4
5
6 electrospun nanofibers. The samples were loaded over sterile filter paper discs (8 mm in
7
8
9 diameter) to obtain a final concentration of 10 mg/disc. About 10 mL of Mueller-Hilton agar
10
11
12 medium was poured into sterile Petri dishes (as a basal layer) followed by 15 mL of seeded
13
14
15 medium previously inoculated with bacterial suspension (100 mL of medium/1 mL of 10^7 CFU)
16
17
18 to attain 10^5 CFU/mL of medium. Sterile filter paper discs loaded with a concentration of 10
19
20
21 mg/mL of electrospun nanofibers were placed on top of Mueller-Hilton agar plates. Filter paper
22
23
24 discs loaded with 10 μ g gentamicin and 10 μ L dimethyl sulfoxide (DMSO, 99.9% purchased
25
26
27 from Sigma-Aldrich) were used as positive and negative controls, respectively. The plates were
28
29
30 kept in the fridge at 5 °C for 2 h. The sample diffusions were incubated at 35 °C for 24 h. The
31
32
33 presence of inhibition zones was measured by a Vernier caliper and recorded and considered an
34
35
36 indication for antibacterial activity.
37
38
39
40
41
42
43
44

45 ***2.12.3. Determination of minimum inhibitory concentrations (MIC's) and minimum***
46
47
48 ***bactericidal concentrations (MBC's)***
49
50

51 MIC is defined as the lowest concentration of the antimicrobial agent that inhibits microbial
52
53
54 growth after 24 h of incubation. The electrospun nanofibers, which exhibit strong antibacterial
55
56
57
58
59
60

1
2
3 activity at 10 mg/mL were manipulated to determine their MIC using the disk diffusion method
4
5
6
7 and evaluate their efficiency in controlling bacterial strains causing food poisoning diseases.
8
9
10 Different concentrations of electrospun nanofiber extract (2.5, 5.0, 10.0, 12.5, and 15.0 mg/mL)
11
12
13 were prepared separately and loaded in their requisite amounts over sterilized filter paper discs (8
14
15
16 mm in diameter). Mueller-Hilton agar was poured into sterile Petri dishes and seeded with
17
18
19 bacterial suspensions of the pathogenic strains. The loaded filter paper discs with different
20
21
22 concentrations of the electrospun nanofibers were placed on top of the Mueller-Hilton agar
23
24
25 plates. The plates were kept in the fridge at 5 °C for 2 h. Then, the samples were incubated at 35
26
27
28 °C for 24 h. The inhibition zones were measured by a Vernier caliper and recorded against the
29
30
31 concentrations of the electrospun nanofibers.
32
33
34
35
36

37 For the MBC's, streaks were taken from the two lowest concentrations of the electrospun
38
39
40 nanofibers plates exhibiting invisible growth (from the inhibition zone of MIC plates) and
41
42
43 subcultures onto sterile Tryptone soya agar (TSA) plates. The plates were incubated at 35 °C for
44
45
46 24 h. Then, they were examined for bacterial growth corresponding to the sample concentration.
47
48
49
50 MBC was taken as the concentration of samples that did not exhibit any bacterial growth on the
51
52
53 freshly inoculated agar plates.
54
55
56
57
58
59
60

3. RESULTS AND DISCUSSION

3.1. Essential oil and solution properties

The extracted oil from dill seeds was pale yellow with a strong characteristic aroma and pleasant odor, and the yield was $3.50 \pm 0.8\%$ (v/w). The yield of DSEO extraction is higher than that of essential oils extracted from dill seeds planted in India, varying between 1.71 and 2.06%.²⁶ The DSEO constituents were identified with GC/MS analysis.

Table 1. Chemical composition of essential oil from dill seeds obtained from Gas chromatography-mass spectrometry analysis.

Peak No.	Compound	Content (%)
1	3,4,4-Trimethyl-3-pentanol	tr
2	Thiocyanic acid, ethyl ester	0.33
3	Camphene	0.43
4	3-Carene	tr
5	β -Phellandrene	tr
6	β -pinene	tr
7	δ -Carene	tr
8	α -Phellandrene	0.42
9	β -Cymene	0.32

10	d-Limonene	36.3
11	γ -Terpinene	2.2
12	Terpinolene	0.46
13	Camphor	0.87
14	Dihydrocarvone	2.6
15	Carvone	13.1
16	Piperitone	16.4
17	Apiol	25.5

tr: trace, relative content < 0.10%.

According to the results in [Table 1](#), 17 components represented 98.93% of the total oil. The major components detected in the oil were d-limonene (36.3%), apiol (25.5%), piperitone (16.4%), and carvone (23.49%). *d*-limonene is a constituent extensively present in essential oils, already identified in commercial DSEO studied by Noumi et al.⁴⁴ The obtained results are in accordance with the literature.^{27,29,45,46}

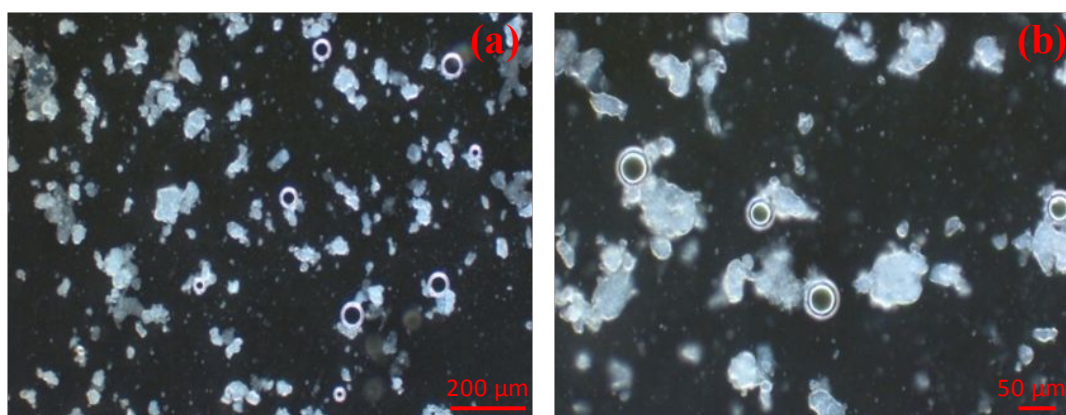
The pH, conductivity, viscosity, and surface tension of prepared solutions and emulsions were determined, and the results are listed in [Table 2](#). The pH value of ≈ 5 indicates that prepared solutions and emulsions are slightly acidic. The viscosity of pure PVA (15% w/v) and the CM/PVA/DSEO emulsion was higher than that of the CM/PVA solution ([Table 2](#)).

Table 2. pH, conductivity, viscosity and surface tension of polymeric solutions and emulsion.

Solution	pH	Conductivity (mS/cm)	Viscosity (mPas ⁻¹)	Surface tension (mN/m)
CM (2% w/v)	5.2	5.8 ± 0.3	8.5± 0.8	24.2± 0.1
PVA (15% w/v)	5.3	42.5 ± 3.2	848.2± 1.2	50.8± 0.4
CM/PVA	5.3	113.2 ± 0.9	421.4± 0.6	46.6± 0.6
CM/PVA/DSEO	5.3	126.5 ± 1.1	627.4± 0.5	26.5± 0.2

The viscosity of the produced polymeric solutions is acceptable to form nanofibers, but a low viscosity of the polymeric solution leads to spindle-shaped beads instead of nanofibers.¹⁶ Also, the high viscosity of a polymeric solution can influence the degree of chain entanglement between polymers and generate large nanofibers. So, the viscosity can reach a critical point, and the nanofiber is generated.¹⁶ In this study, the viscosity of polymeric solutions and emulsions can be used for electrospun nanofibers. The viscosity results agree with those of Rafiq et al.,⁴⁷ who studied the viscosity of PVA/sodium alginate and PVA/sodium alginate loaded with cinnamon, clove, and lavender. The conductivity of the PVA solution increases with increasing carboxylic groups and anionic polyelectrolytes in mucilage polysaccharides and with additions of Tween 80 emulsifier and DSEO. The surface tension of the pure PVA aqueous solution was 50.8 mN/m,

1
2
3 which was higher than the surface tension of CM and oil-containing solutions, which were 46.6
4
5
6
7 and 26.5 mN/m, respectively. It has been observed that adding CM polysaccharides and DSEO
8
9
10 decreases the surface tension. This reduction may be due to the polysaccharide chains' reactivity,
11
12
13 particle size distribution, and strong inter-polymer interactions between emulsion, surfactant, and
14
15
16
17 polysaccharide macromolecules.⁴⁸
18
19
20



35 **Figure 2.** Optical microscopic images of an oil-in-water emulsion of DSEO/CM/PVA: (a) scale
36
37 bars corresponds to 200 μm and (b) scale bars corresponds to 50 μm .
38
39
40
41

42 **Figure 2** shows the optical microscopy images of the oil-in-water emulsion of DSEO in
43
44
45
46 CM/PVA aqueous solution that were taken right after they were made. The O/W emulsion
47
48
49 images show that the oil droplets have been encased as separate spherical globules with a thick
50
51
52 shell (**Figure 2b**). These globules are polydispersed with different diameters, which shows that
53
54
55
56 there are no agglomerates. The average diameter of microcapsules and droplets is between 1 ± 0.4
57
58
59
60

1
2
3
4 μm and $50 \pm 1.2\mu\text{m}$. The emulsification step involves a complex interaction between the oil and
5
6
7 the CM/PVA aqueous phase and produces, with Tween 80, a stable emulsion. The
8
9
10 CM/PVA/DSEO emulsion is more stable than the PVA/thyme essential oil emulsion prepared for
11
12
13 emulsion electrospinning.¹⁷
14
15
16
17

18 **3.2. Fiber morphology and topography**

19
20

21 SEM micrographs of electrospun nanofibers are shown in [Figure 3](#). Electrospinning CM/PVA
22
23
24 and CM/PVA/DSEO emulsions made smooth, uniform nanofibers that were not woven and
25
26
27
28 didn't have any microbeads.
29
30
31
32
33
34
35
36
37
38
39
40
41
42
43
44
45
46
47
48
49
50
51
52
53
54
55
56
57
58
59
60

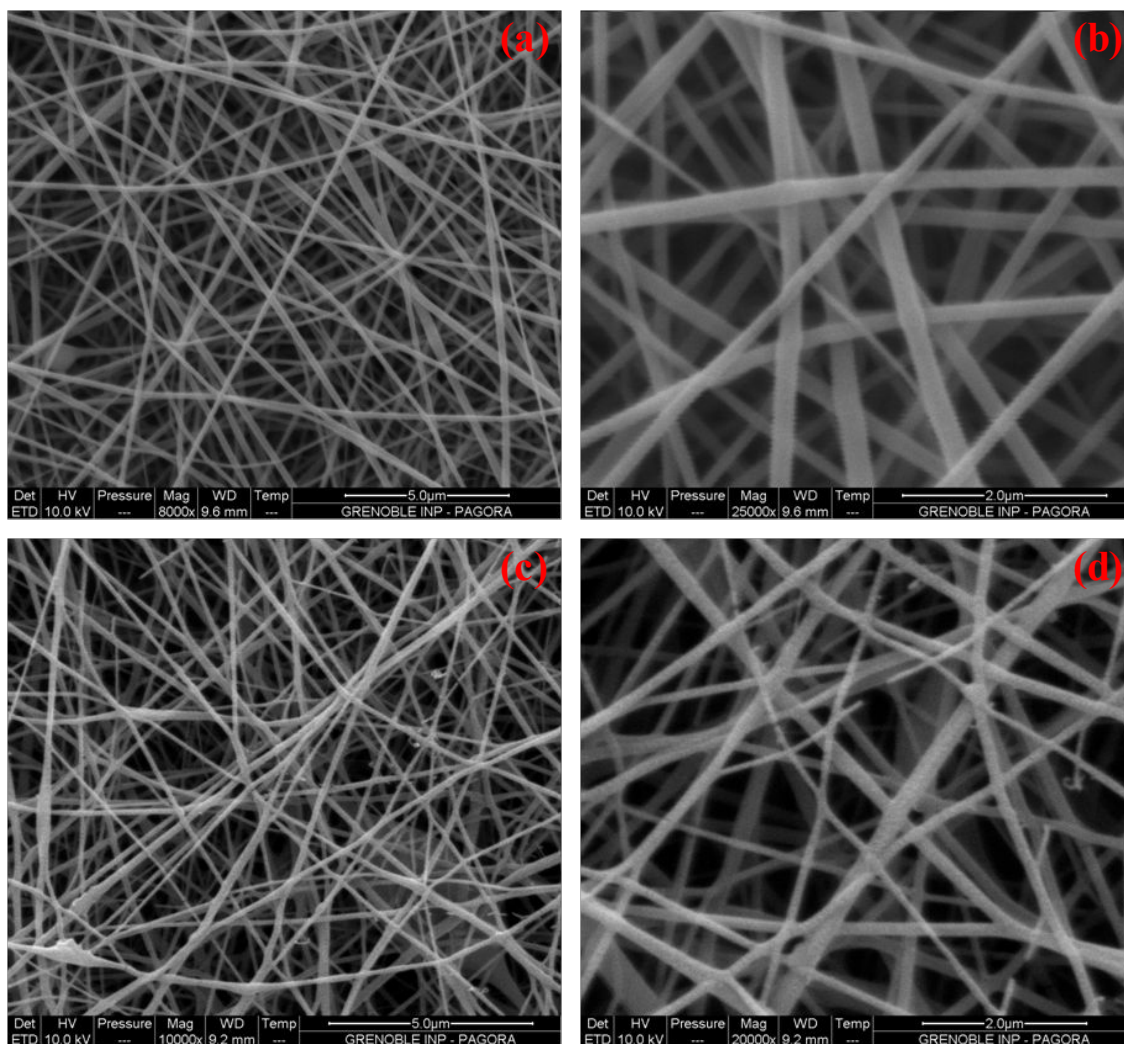


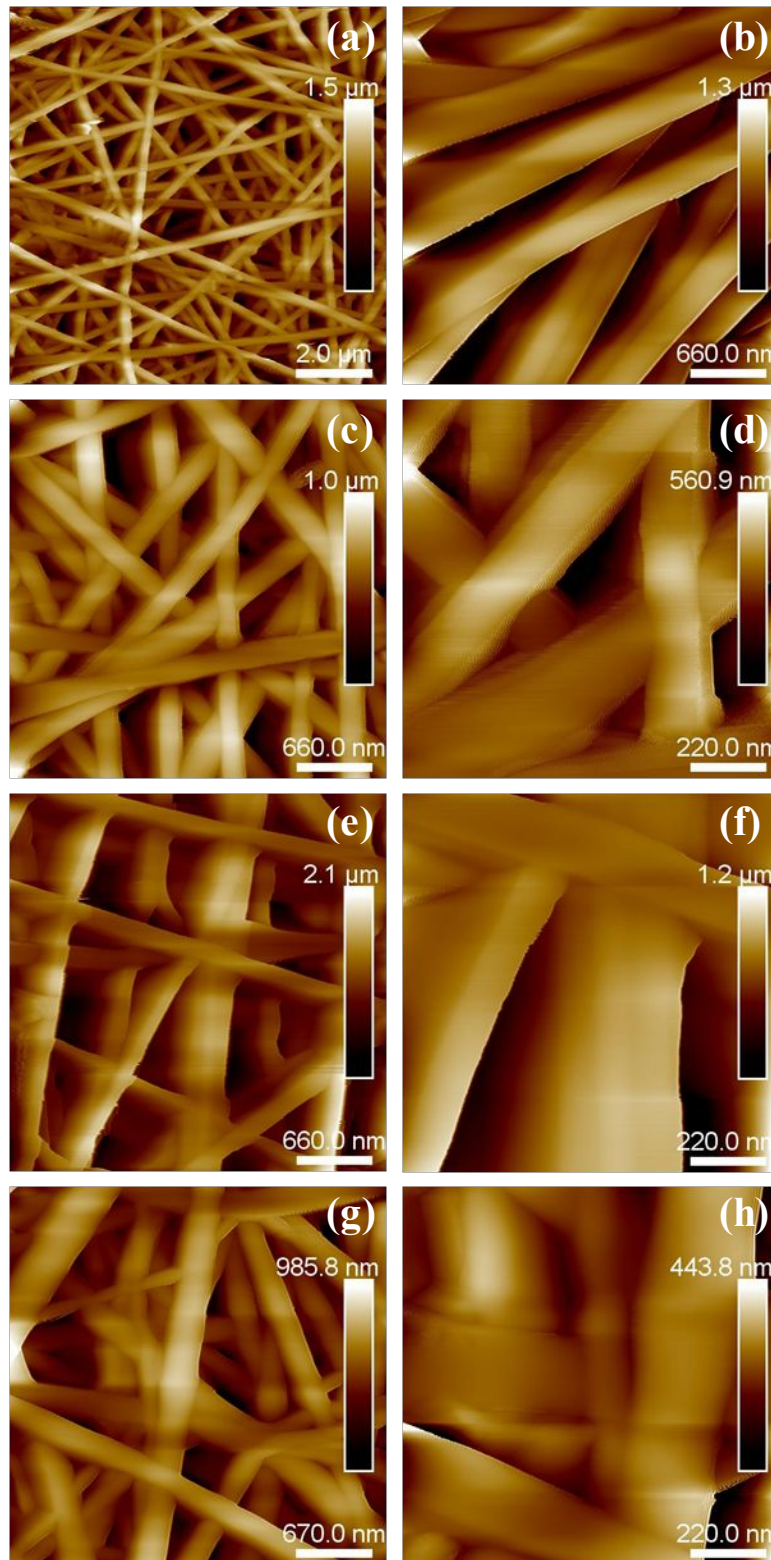
Figure 3. SEM micrographs of: (a-b) CM/PVA electrospun nanofibers [a: 8000 \times and b: 25000 \times] and (c-d) CM/PVA/DSEO electrospun nanofibers [c: 10000 \times and d: 20000 \times].

The CM/PVA electrospun nanofibers had an average diameter of 158 ± 18 nm, whereas that of the loaded electrospun fibers with essential oil was slightly larger, *i.e.* 230 ± 26 nm. The increase in diameter of CM/PVA/DSEO emulsion electrospun nanofibers is probably due to the essential oil encapsulation and incorporation into the nanospun nanofibers. Furthermore, emulsion

1
2
3 electrospinning produced bead-free fibers. In general, the morphology of electrospun fiber is
4
5
6 strongly affected by the viscosity and conductivity of the spinning polymer emulsion, solution,
7
8
9
10 or melt. The large values of viscosity and electrical conductivity in emulsion, compared to
11
12
13 CM/PVA solution (Table 2), improve electrostatic interactions and other types of colloidal
14
15
16 interactions like van der Waals, steric, depletion, and salt-induced attraction between
17
18
19 macromolecules of polymeric solution. The effects of hydrogen bonding and interactions
20
21
22 between polymers lead to broad and uniform nanospun without bead defects during
23
24
25 electrospinning.⁴⁹ Similar morphology has been observed in many other electrospun nanofibers
26
27
28 loaded with different sources of essential oil, such as PVA/cinnamon essential oil/ β -cyclodextrin
29
30
31 electrospun nanofibers,⁵⁰ Polyvinylpyrrolidone/cinnamon essential oil,²³ PVA/gelatin nanospun
32
33
34 loaded with thyme essential oil,⁴⁸ avocado oil in ultrafine zein nanofibers,⁵¹ electrospun
35
36
37 nanofibers of PVA/chitosan functionalized with cabreuva essential oil,¹⁵ zein electrospun
38
39
40 nanofibers loaded with cumin essential oil,²⁴ and costmary essential oil loaded salep-PVA
41
42
43 electrospun.²²
44
45
46
47
48
49

50 AFM is a useful tool for studying the topography of the electrospun nanofibers to further confirm
51
52
53 that they are made from CM-blend PVA and emulsion. It can be seen that the AFM images
54
55
56
57
58
59
60

1
2
3
4 (Figure 4) are in good agreement with the obtained SEM micrographs in terms of fiber
5
6
7 structures. The topographical surfaces show the tubular morphology of all electrospun nanofibers
8
9
10 as reported elsewhere.²⁴
11
12
13
14
15
16
17
18
19
20
21
22
23
24
25
26
27
28
29
30
31
32
33
34
35
36
37
38
39
40
41
42
43
44
45
46
47
48
49
50
51
52
53
54
55
56
57
58
59
60



1
2
3
4 **Figure 4.** AFM images of the surface topography of: (a–d) CM/PVA electrospun nanofibres [a:
5
6 scale bars 2 μm , b: scale bars 660 nm, c: scale bars 660 nm and d: scale bars 220 nm] and (e–h)
7
8
9
10 CM/PVA/DSEO electrospun nanofibres [e: scale bars 660 nm, f: scale bars 220 nm, j: scale bars
11
12
13
14 670 nm and h: scale bars 220 nm].

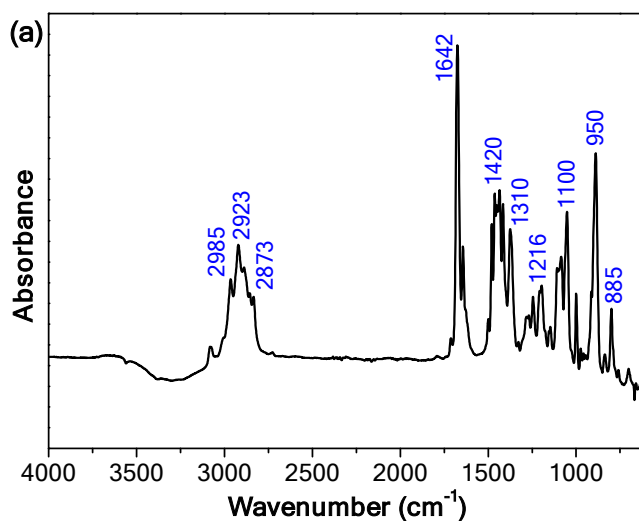
15
16
17
18 The topography image of CM/PVA electrospun nanofibers reveals a fibrillar structure with
19
20
21 rough, laminated, and cross-linked nanospun fibers forming a nonwoven mat structure (Figure 4
22
23
24 a-d). The diameter of electrospun nanofibers increases when dill seed essential oil is added. It is
25
26
27 confirmed that surface roughness increases with increasing electrospun fiber diameter.⁵² The
28
29
30
31 CM/PVA/DSEO regenerating fibers with encapsulated oil seem larger with entangled edges.
32
33
34 Similar topography has been reported in other electrospun fabrics produced with polysaccharide-
35
36
37
38 essential oil emulsions.^{24,53}

3.3. ATR-FTIR

39
40
41
42
43
44
45 ATR-FTIR spectra of the extracted dill seed essential oil obtained by hydrodistillation (Figure
46
47
48
49 5a) show the presence of the characteristic vibration bands of the main components of DSEO. It
50
51
52 can be observed that the peaks at 1310, 1216, 950, and 885 cm^{-1} are attributed to the double
53
54
55 bonds in α -limonene as a major compound.^{54,55} Also, a characteristic band at 1642 cm^{-1}
56
57
58
59
60

1
2
3 corresponds to the stretching band of C=C as a functional group in *d*-limonene, apiol, carvone,
4
5
6
7 pinene, etc....⁴⁸ The bands are characteristic of the terpenes found in essential oils.⁵⁶ Other bands
8
9
10 are observed between 3100 and 2850 cm⁻¹, related to -CH, -CH₂ and -CH₃ stretch vibrations.
11
12

13 The ATR-FTIR spectra of extracted CM are shown in Figure 5b, exhibiting a spectrum
14
15 similar to that reported by other authors for cactus polysaccharide. The characteristic broadband
16
17 at 3300 cm⁻¹ corresponds to the stretching of -OH groups of the polysaccharides in mucilage.⁵⁷
18
19
20 The small band situated at 2900 cm⁻¹ is attributed to the -CH₂ group vibration of the pyranose
21
22
23
24 backbone.⁵⁸ The band occurring at 1763 cm⁻¹ is related to the C=O bonds.⁵⁹
25
26
27
28
29



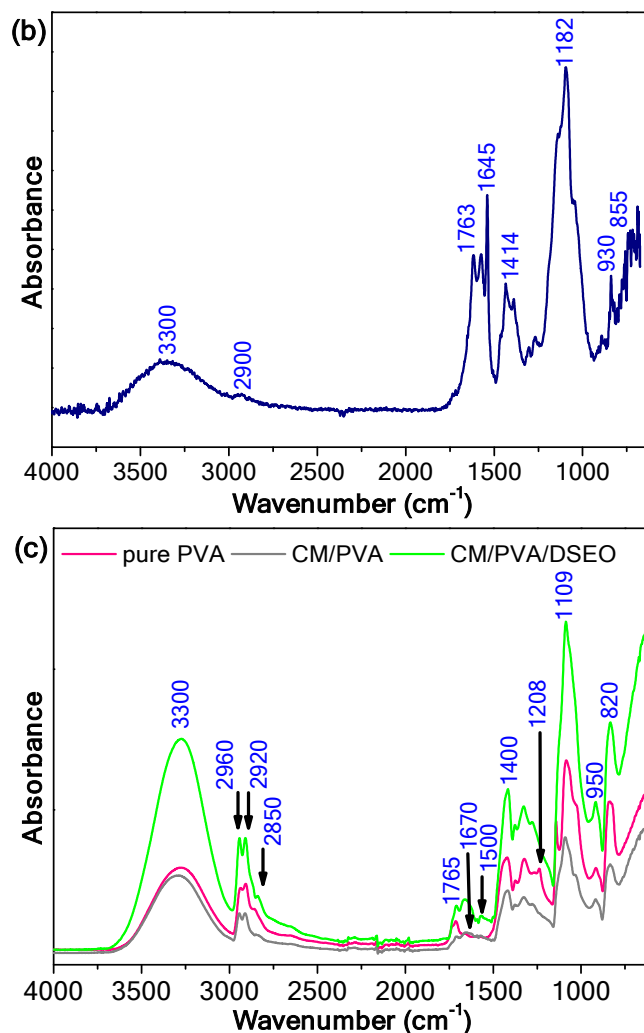


Figure 5. ATR-FTIR spectra of: (a) DSEO, (b) CM and (c) pure PVA, CM/PVA and CM/PVA/DSEO electrospun nanofibres.

The two bands observed at 1645 and 1414 cm⁻¹ are attributed to the asymmetric and symmetric stretching vibrations of the -COO⁻ of the salts of the carboxylic acids, probably the uronic acid in mucilage.⁶ The characteristic band shown at 1182 cm⁻¹ corresponds to the C-O stretching vibration of the pyranose ring of mucilage.^{57,60} The bands observed at 930 and 855 cm⁻¹ are

1
2
3 attributed to the presence of α and β -D-glucose configurations.⁵⁷ The studied spectra reveal that
4
5
6
7 cactus mucilage is rich in polysaccharides, which can form new links with other polymers.
8
9

10 **Figure 5c** shows the chemical functional profiles for the pure PVA, CM/PVA and
11
12
13 CM/PVA/DSEO electrospun nanofibers. The spectra of the analyzed electrospun nanofibers did
14
15
16
17 not show significant changes when compared to those of pure PVA. For pure PVA, the
18
19
20 broadband absorption at 3300 cm^{-1} corresponds to hydroxyl stretching vibrations for the
21
22
23 intermolecular and intramolecular hydrogen bonds. The bands at 2960 and 2920 cm^{-1} are
24
25
26 attributed to the C–H stretching vibrations of alkyl groups, and the peaks in the region between
27
28
29 1765 and 1700 cm^{-1} are assigned to the non-hydrolyzed vinyl acetate groups (C=O stretching).⁵³
30
31
32
33 Other peaks at 1400 , 1109 , 950 , and 820 cm^{-1} are related to the CH_2 , C–O–C and C–C bonds,
34
35
36 respectively.⁶¹ The spectra of CM/PVA electrospun nanofibers revealed increased absorption
37
38
39 intensities at 1670 and between 1100 and 1200 cm^{-1} , corresponding to both carbonyl and carbon-
40
41
42 oxygen stretching frequencies, respectively, associated with the polysaccharide nature of
43
44
45 mucilage.⁶² In the spectra of CM/PVA/DSEO electrospun nanofibers, the addition of DSEO did
46
47
48
49 not cause any significant changes compared with the spectra of CM/PVA electrospun nanofibers.
50
51
52
53 It could be seen that the DSEO and CM/PVA polymers are intermolecularly bound, which
54
55
56
57
58
59
60

1
2
3 confirms the encapsulation of oil in the CM-blend PVA nanofiber structure. These findings agree
4
5
6
7 with the other studies in the literature.^{17,22,50,53,62}
8
9

11 3.4. Thermal properties

12
13
14 The TGA/HF profiles of DSEO, CM, pure PVA, CM/PVA and CM/PVA/DSEO electrospun
15
16
17 nanofibers were recorded at temperatures ranging from 30 to 700 °C (Figure 6). The TGA of
18
19
20 DSEO is presented in Figure 6a. As can be seen, DSEO has a typical TGA profile with only one
21
22
23 evaporation stage starting at 70 °C and finishing at 200 °C, with a maximum weight loss of
24
25
26
27 99.6wt% around 110 °C. From the HF curve, it can be seen that DSEO absorbed energy to assess
28
29
30 the evaporation. The thermal behavior of DSEO is similar to that of the essential oil of citrus
31
32
33 limon⁵⁰ and greater than that of cinnamon essential oil, which has an evaporation/degradation
34
35
36
37 temperature between 63 °C and 119 °C.¹⁰
38
39
40

41 The TGA curve of CM (Figure 6b) revealed three essential degradation zones. The first zone
42
43
44 is kept between 30 and 150 °C, degrades about 12 wt% of CM, and involves the evaporation of
45
46
47 the moisture.^{36,63} The second zone ranges between 150 and 490 °C and is attributed to the
48
49
50 mucilage's thermal decomposition with a loss of 40 wt%. A slight thermal stability appears
51
52
53
54 between 150 and 250 °C due to gelatinization followed by branch breakage.^{36,38} When the CM is
55
56
57
58
59
60

1
2
3 heated, thermal decomposition occurs in this zone, involving the continuous and slow
4
5
6 decomposition of carbonaceous matter. The HF curve of CM shows the combustion peak, which
7
8
9 releases a high quantity of energy during the decomposition reaction. The third zone occurs from
10
11
12
13 490 to 700 °C, in which losses of 18 wt% follow slight thermal stability and involve broken
14
15
16 chains, residual branches of polysaccharides, and some crystalline structure degradations.⁶⁴
17
18
19 Beyond 680 °C, the slight stability revealed the ash content.
20
21
22

23
24 The TGA curve of PVA displays two thermal events (Figure 6c). The first thermal
25
26 decomposition zone occurs between 30 and 210 °C, with losses of about 8 wt%. It involves the
27
28 evaporation of physically weakly bound water and chemically strongly bound water due to the
29
30 relaxation of the crystalline domains in PVA.⁶⁵ The second transition zone ranges from 210 to
31
32
33 530 °C and loses about 92 wt%. The total weight loss of pure PVA was reached at 490 °C. This
34
35
36 event is confirmed by the typical prominent peak observed in the HF curve (Figure 6d). This
37
38
39 significant transition is associated with the degradation of the PVA polymeric backbone caused
40
41
42
43
44
45
46
47 by the melting of the crystalline domains as hydrogen bonds begin to break.^{31,65}
48
49
50
51
52
53
54
55
56
57
58
59
60

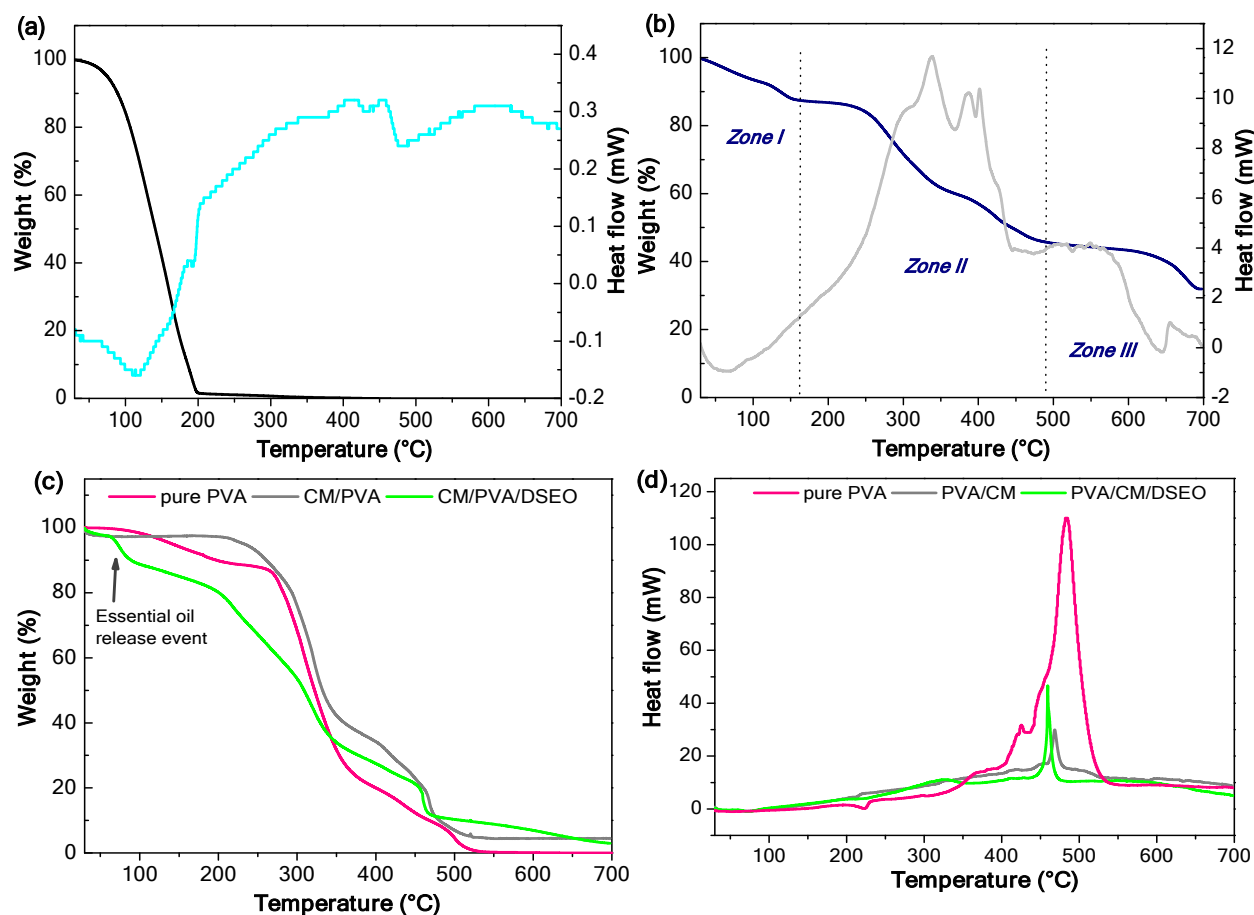


Figure 6. TGA thermograms of: (a) TGA/HF curves of DSEO, (b) TGA/HF of CM, (c) TGA and (d) HF curves of pure PVA, CM/PVA and CM/PVA/DSEO electrospun nanofibres.

The TGA curve of CM/PVA displays two thermal events (Figure 6c). The first step of degradation ranges from 30 to 120°C; losses of about 3 wt% are attributed to the evaporation of moisture at 80 °C (Figure 6d). The second step starts from 120 °C to 530 °C and causes a degradation of about 92 wt%. Thermal stability occurs in the region of 120 and 230 °C related to the CM enhancement of PVA electrospun; similar stability is shown for CM in Figure 6b. The

1
2
3
4 second step of degradation includes two transitions. The first transitional degradation began at
5
6
7 250 °C and was achieved at 350 °C attributed to the heating degradation of the PVA side chain.⁶²
8
9

10 The second transition occurs from 350 to 530 °C and corresponds to continuous mucilage
11
12
13 polysaccharide degradation. The higher thermal stability of CM/PVA electrospun nanofibers
14
15
16 compared to pure PVA might be due to the hydrogen bonding interaction between the hydroxyl
17
18
19 groups of CM and PVA and the compactness of the chain. The CM/PVA electrospun nanofibers
20
21
22 produced in this study are more thermally stable than the basil seed mucilage/PVA electrospun
23
24
25
26
27 nanofibers⁴⁹ and flaxseed mucilage/PVA nanofibers.⁶⁶
28
29

30 The TGA curve of CM/PVA/DSEO electrospun nanofibers shows that the weight loss occurred
31
32
33 mainly in two stages with significant changes in CM/PVA electrospun nanofibers (Figure 6c).
34
35
36

37 From 30 to 120 °C, the evaporation of residuals has occurred, and the oil releases when heated
38
39
40 above 70 °C. The second stage of degradation starts at 120 to 480°C. In this region, two thermal
41
42
43 transitions of degradation appeared. The first transition occurs between 120 and 350°C attributed
44
45
46 to PVA backbone polymer degradation, while the second transition ranges from 350 to 480°C
47
48
49 and corresponds to polysaccharide degradation. After 480°C, an ultimate line of weight loss was
50
51
52
53
54 observed to slow down, related to the presence of ash naturally present in cactus mucilage
55
56
57
58
59
60

1
2
3 polysaccharides. The findings suggest that adding cactus mucilage enhances the thermal stability
4
5
6 of PVA electrospun nanofibers and that the DSEO is successfully encapsulated in the nanospun
7
8
9 fibers. The thermal behavior of CM/PVA/DSEO electrospun nanofibers is more significant than
10
11
12 that of PVA/cinnamon essential oil and PVA/cinnamon essential oil/ β -cyclodextrin electrospun
13
14
15 nanofibers.⁵⁰ The remarkable difference in the TGA curves of DSEO, CM, pure PVA and
16
17
18 electrospun nanofibers revealed that the chemical interaction among the two polymers with
19
20
21
22
23 DSEO had occurred successfully in the electrospun nanofibers.
24
25
26
27

28 **3.5. Contact angle**

29
30
31 **Figure 7** shows how the water contact angles of CM/PVA and CM/PVA/DSEO electrospun
32
33
34 fibers change over time. T_0 is the initial contact time of the water droplet and T_f is the time when
35
36
37 the analysis is over. All the water contact angles were < 90 , indicating the hydrophilic property
38
39
40 of the produced CM-blend PVA electrospun nanofibers. Hydrophilic surfaces present better
41
42
43
44
45 affinity for cells than hydrophobic surfaces.⁶⁷
46
47
48
49
50
51
52
53
54
55
56
57
58
59
60

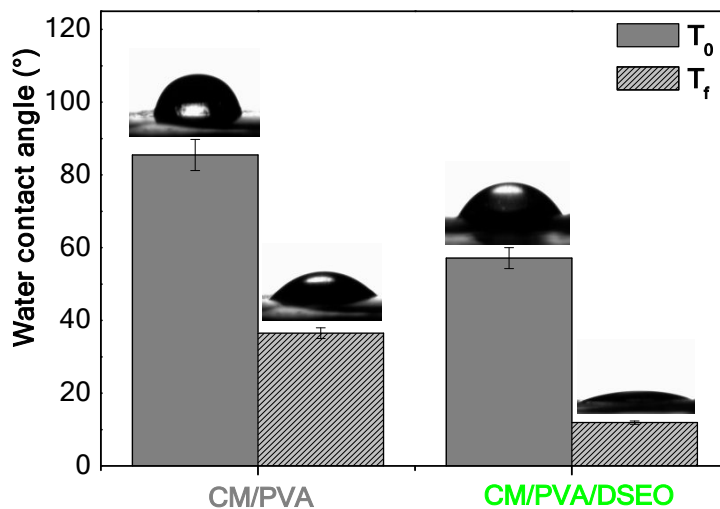


Figure 7. Water contact angles of CM/PVA and CMPVA/DSEO electrospun nanofibers.

The water contact angles of CM/PVA and CM/PVA/DSEO electrospun nanofibers were 86° and 58° at T_0 , which were reduced to 37° and 12°, respectively. The high water contact angle of the analyzed specimens can be explained by the rough surface of electrospun nanofibers. The recorded water contact angles of blended PVA electrospun nanofibers were observed to be greater than those of neat PVA electrospun fibers.¹¹ It reveals that adding cactus carbohydrates and essential oils to electrospun nanofibers can significantly reduce the value of the water contact angle. Moreover, the recorded digital pictures show clearly that the water contact angle of the electrospun nanofibers at T_0 has a better resistance against water than that of the emulsion-based electrospun nanofibers. At T_f , the reduction in contact angle values depends on the polar hydroxyl group of the formulated nanospun, especially the hydroxyl groups of cactus mucilage,

1
2
3
4 as well as the electrospun fibers partial dissolution during the water contact angle test. It means
5
6
7 CM/PVA and CM/PVA/DSEO electrospun nanofibers have water absorbency as required for an
8
9
10 ideal scaffold, which must be used in tissue wound dressings^{11,50} and smart food packaging
11
12
13 applications.⁹
14
15
16
17

18 **3.6. Encapsulation efficiency**

19
20
21 EE is one of the critical parameters in encapsulation technology; it was used to determine the
22
23
24 efficiency of the electrospun fiber in the entrapment of the oil.^{24,68} The EE of DSEO in CM/PVA
25
26
27 electrospun nanofibers was 100%. The EE of DSEO in CM/PVA electrospun nanofibers is
28
29
30 greater than those of thyme essential oil in zein with an EE of 75.23±16.4%,²¹ rosemary ethanoic
31
32
33 extract in PVA fibers with a retention efficiency of 88%,⁶⁹ and costmary essential oil in salep-
34
35
36 PVA with an EE ranging between 93.21–96.62%.²² These findings confirm the efficacy of PVA
37
38
39 blended with cactus mucilage in the electrospinning method and for encapsulating essential oils.
40
41
42
43
44
45

46 **3.7. Essential oil release**

47
48
49 The release profiles of free DSEO and DSEO encapsulated in electrospun nanofibers were
50
51
52 studied for 96 and 552 h, respectively. [Figure 8](#) shows the release process of free DSEO which
53
54
55 reveals that after 8 h, the release process started to increase gradually and reached 96 h to
56
57
58
59
60

complete the total release. The free DSEO release profile is considered more stable than that of free orange essential oil, which completes its total release after 72 h.²⁰

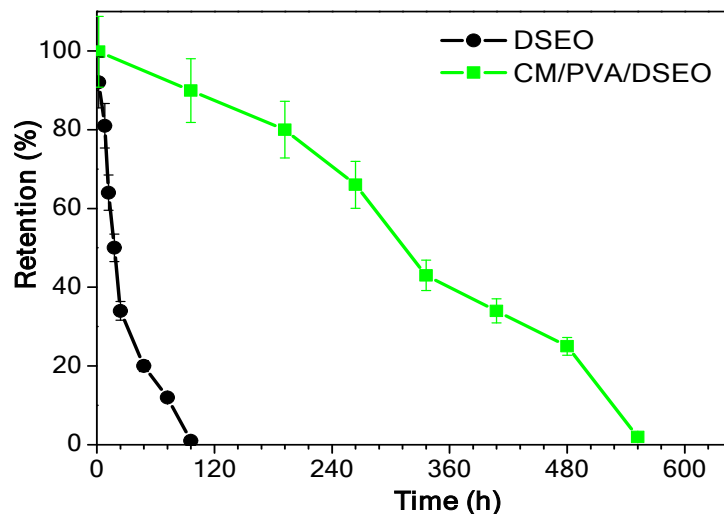


Figure 8. The release profile of free and loaded DSEO in electrospun nanofibers during 552 h (23 days).

The release process of encapsulated essential oil from electrospun nanofibers proves the gradual release process. This slower release of DSEO seems to be due to the gradual release of entrapped material, which confirms that the DSEO is encapsulated into the nanospun fibers. These findings confirm that the DSEO release took place in the fibers, suggesting that the blending of CM with PVA promotes a more controlled release. The CM/PVA electrospun fibers are considered better carriers for essential oils than the electrospun poly (lactic acid) nanofiber loaded with *Zingiber*

1
2
3 *Cassumunar Roxb* essential oil, reaching their maximum release of about 80% after 12 h⁷⁰ and
4
5
6
7 almost 50% of the nanoemulsified *Cuminum cyminum* essential oil was released from the
8
9
10 electrospun *Plantago psyllium* L. seed gum/gelatin nanofibers within the first 12 hours and
11
12
13 reached zero after 36 h.⁷¹ It means CM/PVA/DSEO electrospun nanofibers have a slow release
14
15
16
17 process for essential oils and are suitable for innovative active packaging and pharmaceutical
18
19
20 uses.
21
22
23

24 3.8. Anti-bacterial activity

25
26
27
28 The electrospun nanofibers were studied to assess their antibacterial activity against food-
29
30
31 poisoning bacteria, including two strains of Gram-positive bacteria (*Staphylococcus aureus* and
32
33
34 *Bacillus cereus*) and three strains of Gram-negative bacteria (*Pseudomonas aeruginosa*,
35
36
37 *Salmonella typhi*, and *Escherichia coli*) using the disc diffusion method, and the obtained results
38
39
40
41 were summarized in [Table 3](#).
42
43
44
45

46 **Table 3.** Antimicrobial test of CM/PVA and CM/PVA/DSEO (10 mg/mL) against some
47
48
49 bacterial strains of food poisoning diseases.
50
51
52

Bacterial strains	Inhibition zones (mm)
-------------------	-----------------------

		CM/PVA	CM/PVA/DSEO	Gentamicin (10 µg/mL)	DMSO
Gram (-ve) PB	<i>Pseudomonas aeruginosa</i>	14.1±1.3	15.5±2.4	16.3±1.1	NI
	<i>Salmonella typhi</i>	13.9±2.5	12.4±1.7	16.1±1.8	NI
	<i>Escherichia coli</i>	12.9±2.6	15.1±0.7	15.8±0.6	NI
Gram (+ve) PB	<i>Staphylococcus aureus</i>	15.3±2.4	16.1±2.1	17.4±0.9	NI
	<i>Bacillus cereus</i>	14.2±1.1	14.9±3.3	15.4±1.1	NI

PB: Pathogenic Bacteria; NI: Non inhibition

Disks containing DMSO had no inhibitory effect, while gentamicin disks had an inhibitory effect on *B. cereus* and *E. coli*. The results obtained by agar disk diffusion revealed that the studied samples were potentially effective in suppressing the microbial growth of food-poisoning bacteria with varying potency. DSEO-loaded CM/PVA was the most effective nanofiber in retarding the microbial growth of all pathogenic bacteria tested at a concentration of 10 mg/mL. It appears that *E. coli* is the most resistant to CM/PVA, while *S. typhi* is the second most resistant. This is due to the nature of mucilage polysaccharides, which have good resistance against bacterial growth, unlike pure PVA, which has no inhibitory effect on bacterial growth.⁷² This result is greater than that reported for nanofibers of chia seed mucilage and polyvinyl alcohol, which have no antibacterial properties.¹⁶ However, with CM/PVA/DSEO, *S. typhi* is the

1
2
3 most resistant, followed by *B. cereus*. On the other hand, *S. aureus* and *P. aeruginosa* are the
4
5
6 most sensitive strains to both types of electrospun nanofibers. CM/PVA electrospun nanofibers
7
8
9 loaded with 4% DSEO had the highest antibacterial activity compared to that reported for
10
11
12 electrospun *Plantago psyllium* L. seed gum/gelatin nanofibers incorporated with 3% *Cuminum*
13
14
15
16
17 *cuminum* essential oil, which also has an inhibitory effect on the growth of *S. aureus*.⁷¹
18
19
20 Furthermore, The improved antimicrobial activity of nanofibers loaded with essential oil is
21
22
23 significantly due to the existence of antibacterial active compounds in DSEO, essentially d-
24
25
26 limonene, apiol, piperitone, and carvone (Table 1). *d*-limonene is the main compound present in
27
28
29 DSEO; it has great applications in antibacterial and food preservation due to its bactericidal
30
31
32 activity, safety, and low toxicity.⁷²⁻⁷⁴ Also, DSEO has an important antibacterial effect against
33
34
35
36
37 foodborne pathogenic bacteria.⁴⁴
38
39

40 The MIC's of the CM/PVA and CM/PVA/DSEO nanofibers were determined by disc diffusion
41
42
43 method to evaluate their bacteriostatic and bactericidal properties, and the obtained results are
44
45
46 reported in Table 4. The inhibitory effect of CM/PVA/DSEO started at 2.5 mg/mL with
47
48
49 inhibition zones of 9.3 and 8.4 mm against *S. aureus* and *P. aeruginosa* while CM/PVA/DSEO
50
51
52
53
54 nanofibers suppressed the bacterial growth of these strains at a concentration of 2.5 mg/mL with
55
56
57
58
59
60

1
2
3 inhibition zones of 6.8 and 7.6 mm, respectively. The MBC's were confirmed by the absence of
4
5
6
7 bacterial growth in the tested strains streaked from the inhibition zone corresponding to their
8
9
10 lowest MIC's. The CM/PVA nanofibers showed potentially bactericidal activity against *S. aureus*
11
12
13 and *P. aeruginosa* with a MBC of 5 mg/mL whereas the MBC of CM/PVA/DSEO reached 10
14
15
16 mg/mL exceptionally for *P. aeruginosa* which is less sensitive with a MBC in the range of 12.5
17
18
19
20 mg/mL.
21
22
23

24 **Table 4.** MIC's of the CM/PVA and CM/PVA/DSEO electrospun nanofibers against *S. aureus*
25 and *P. aeruginosa*.
26
27

Sample	Conc. (mg/mL)	Inhibition zones (mm)	
		Gram (+ve) PB	Gram (-ve) PB
		<i>S. aureus</i>	<i>P. aeruginosa</i>
CM/PVA	2.5	9.3±0.97	8.4±1.20
	5	11.3±1.10	11.3±1.10
	10	15.4±2.60	14.1±1.30
	12.5	19.4±0.92	16.3±0.67
	15	19.5±2.10	19.3±0.90
CM/PVA/DSEO	2.5	6.8±1.25	7.6±1.26
	5	9.6±1.42	10.5±0.95
	10	16.1±2.10	15.5±2.40

12.5	19.6±1.60	20.1±1.90
15	22.6±2.20	22.4±2.60

PB: Pathogenic Bacteria

Generally, it has been reported that the MIC and MBC of *Anethum graveolens L.* varied depending upon the plant and pathogen strains as well as the solvent system of active compound extractions.²⁸ These results prove the good synergy between CM and DSEO only against bacteria, compared to that of DSEO, which has MIC and MBC values ranging from 0.048 to 0.097 mg/mL and 12.5 to >50 mg/mL, respectively, for the bacterial strains.⁴⁴ The studied MIC and MBC of the electrospun nanofibers suggest that they can be used to control and take necessary measures to prevent foodborne bacteria and food poisoning. Thus, the encapsulation of DSEO in electrospun nanofibers significantly proves its effectiveness to be used as a considerable natural antibacterial agent and could be exploited as a natural preservative in the food industry owing to its efficacy and safety.⁴⁴

4. CONCLUSION

The present study investigated the potential of cactus PVA and PVA electrospun nanofibers as wall materials for the encapsulation of DSEO via electrospinning. The GC/MS analysis of the

1
2
3 extracted DSEO identified four major components: α -limonene, apiol, piperitone, and carvone.
4
5
6

7 The spinning solution and emulsion prove their suitability and efficiency to produce electrospun
8
9
10 nanofibers. The optical microscopy of the CM/PVA/DSEO emulsion shows that it contains
11
12
13 polydispersed microcapsules of various sizes. The morphology of the electrospun nanofibers
14
15
16 produced without and with essential oil revealed that adding essential oil leads to a slight
17
18
19 increase in fiber diameters. Similar findings are proven with AFM. A thermal investigation
20
21
22 revealed the enhancement of PVA's thermal stability when blended with CM. The water contact
23
24
25 angle measurements confirmed that formulated electrospun nanofibers have water absorbency.
26
27
28 The encapsulation efficiency and oil release of the free and encapsulated oils prove the suitability
29
30
31 of CM and PVA blends as effective core shells for protecting essential oils or other bioactive
32
33
34 compounds. The CM/PVA nanofibers containing DSEO showed enhanced antibacterial
35
36
37 properties against *S. typhi* and *B. cereus*. These results confirm that these nanofibers could be
38
39
40 used as a promising controlled delivery system for value-added smart food packaging
41
42
43 applications, encapsulation technologies, biomedical, and pharmaceutical applications.
44
45
46
47
48
49
50

51 AUTHOR INFORMATION

52 53 54 55 **Corresponding Author** 56 57 58 59 60

1
2
3 * **Younes Moussaoui** – University of Gafsa, Faculty of Sciences of Gafsa, Tunisia; University of
4
5
6
7 Sfax, Faculty of Sciences of Sfax, Organic Chemistry Laboratory (LR17ES08), Tunisia;
8
9
10 <https://orcid.org/0000-0003-0329-2443>; Email: y.moussaoui2@gmx.fr
11
12

13 14 **Authors**

15
16
17
18 **Faten Mannai** – University of Gafsa, Faculty of Sciences of Gafsa, Laboratory for the
19
20
21 Application of Materials to the Environment, Water and Energy (LR21ES15), Tunisia
22
23

24
25 **Hanedi Elhleli** – University of Gafsa, Faculty of Sciences of Gafsa, Laboratory for the
26
27
28 Application of Materials to the Environment, Water and Energy (LR21ES15), Tunisia
29
30

31
32 **Anouar Feriani** – University of Gafsa, Faculty of Sciences of Gafsa, Laboratory of
33
34
35 Biotechnology and Biomonitoring of the Environment and Oasis Ecosystems, Tunisia
36
37
38

39
40 **Issei Otsuka** – University of Grenoble Alpes, CNRS, CERMAV, Grenoble, F-38000, France
41
42

43
44 **Mohamed Naceur Belgacem** – University of Grenoble Alpes, CNRS, Grenoble INP, LGP2,
45
46
47 Grenoble, F-38000, France
48
49

50 51 **Author Contributions**

1
2
3
4 The manuscript was written through contributions of all authors. All authors have given approval
5
6
7 to the final version of the manuscript. F.M.: conceptualization, investigation, data curation,
8
9
10 writing — original draft preparation, methodology. H.E.: resources, methodology, investigation,
11
12
13 conceptualization. A.F.: data curation, investigation. I.O.: material preparation,
14
15
16 conceptualization. M.N.B.: methodology, formal analysis, supervision, writing— review and
17
18
19 editing. Y.M.: methodology, supervision, visualization, writing— review and editing
20
21
22
23
24

25 **Funding Sources**

26
27
28 This research has been funded by Ministry of Higher Education, Scientific Research and
29
30
31 Technology, Tunisia through project number PAQ-PAES/T2-PAES 2-15.
32
33
34
35

36 **Notes**

37
38
39 The authors declare no competing financial interest.
40
41
42
43

44 **ACKNOWLEDGMENT**

45
46
47 The authors acknowledge Sami Halila and Laurine Buon from CNRS, CERMAV, University of
48
49
50 Grenoble Alpes, who analyzed oil with gas chromatography/mass spectrometry.
51
52
53
54

55 **ABBREVIATIONS**

1
2
3 AFM, atomic force microscopy; ATR, attenuated total reflectance; *B. cereus*, *Bacillus cereus*;
4
5
6
7 CM, cactus mucilage; DMSO, dimethyl sulfoxide; DSEO, dill seed essential oil; *E. coli*,
8
9
10 *Escherichia coli*; EE, encapsulation efficiency; HF, heat flow; MBC's, minimum bactericidal
11
12
13 concentrations; MIC's, minimum inhibitory concentrations; NI, Non inhibition; NIST, National
14
15
16 Institute of Standards and Technology; PVA, polyvinyl alcohol; *P. aeruginosa*, *Pseudomonas*
17
18 *aeruginosa*; PB, pathogenic bacteria; *S. aureus*, *Staphylococcus aureus*; *S. typhi*, *Salmonella*
19
20 *typhi*; SEM, scanning electron microscopes; TGA, thermogravimetric analysis.
21
22
23
24
25
26
27

28 REFERENCES

- 29
30
31 (1) Anaya-Mancipe, J. M.; Queiroz, V. M.; dos Santos, R. F.; Castro, R. N.; Cardoso, V. S.;
32
33
34 Vermelho, A. B.; Dias, M. L.; Thiré, R. M. Electrospun Nanofibers Loaded with *Plantago major*
35
36
37 L. Extract for Potential Use in Cutaneous Wound Healing. *Pharmaceutics* **2023**, *15* (4), No.
38
39
40
41 1047.
42
43
44
45 (2) Elnabawy, E.; Sun, D.; Shearer, N.; Shyha, I. Electro-Blown Spinning: New Insight into the
46
47
48 Effect of Electric Field and Airflow Hybridized Forces on the Production Yield and
49
50
51 Characteristics of Nanofiber Membranes. *J. Sci. Adv. Mater. Devices* **2023**, *8* (2), No. 100552.
52
53
54
55
56
57
58
59
60

1
2
3
4 (3) Tahir, M.; Vicini, S.; Sionkowska, A. Electrospun Materials Based on Polymer and
5
6
7 Biopolymer Blends—A Review. *Polymers* **2023**, *15*(7), No. 1654.

8
9
10
11 (4) Shi, S.; Si, Y.; Han, Y.; Wu, T.; Iqbal, M. I.; Fei, B.; Li, R. K. Y.; Hu, J.; Qu, J. Recent
12
13
14 progress in protective membranes fabricated via electrospinning: advanced materials, biomimetic
15
16
17 structures, and functional applications. *Adv. Mater.* **2022**, *34*(17), No. 2107938.

18
19
20
21 (5) Han, W.; Wang, L.; Li, Q.; Ma, B.; He, C.; Guo, X.; Nie, J.; Ma, G. A Review: Current
22
23
24 Status and Emerging Developments on Natural Polymer Based Electrospun Fibers. *Macromol.*
25
26
27 *Rapid Commun.* **2022**, *43*(21), No. 2200456.

28
29
30
31 (6) Poshina, D.; Otsuka, I. Electrospun Polysaccharidic Textiles for Biomedical Applications.
32
33
34
35
36 *Textiles* **2021**, *1*(2), 152–169.

37
38
39
40 (7) Otsuka, I.; Njinang, C. N.; Borsali, R. Simple fabrication of cellulose nanofibers via
41
42
43 electrospinning of dissolving pulp and tunicate. *Cellulose* **2017**, *24*(8), 3281–3288.

44
45
46
47 (8) Ajith, G.; Tamilarasi, G. P.; Sabarees, G.; Gouthaman, S.; Manikandan, K.; Velmurugan,
48
49
50
51 V.; Alagarasamy, V.; Solomon, V. R. Recent Developments in Electrospun Nanofibers as
52
53
54

1
2
3
4 Delivery of Phytoconstituents for Wound Healing. *Drugs and Drug Candidates* **2023**, *2* (1), 148–
5
6
7 171.

8
9
10 (9) Arik, N.; Horzum, N.; Truong, Y. B. Development and Characterizations of Engineered
11
12 Electrospun Bio-Based Polyurethane Containing Essential Oils. *Membranes* **2022**, *12* (2), No.
13
14
15
16
17
18 209.

19
20
21 (10) de Souza, A. G.; Barbosa, R. F. D. S.; Quispe, Y. M.; Rosa, D. D. S. Essential oil
22
23 microencapsulation with biodegradable polymer for food packaging application. *J. Polym.*
24
25
26
27
28
29 *Environ.* **2022**, *30*(8), 3307–3315.

30
31
32 (11) Salam, A.; Khan, M. Q.; Hassan, T.; Hassan, N.; Nazir, A.; Hussain, T.; Azeem, M.; Kim,
33
34 I. S. In-vitro assessment of appropriate hydrophilic scaffolds by co-electrospinning of poly (1,4
35
36
37
38
39
40
41
42
43
44
45
46
47
48
49
50
51
52
53
54
55
56
57
58
59
60
I. S. In-vitro assessment of appropriate hydrophilic scaffolds by co-electrospinning of poly (1,4
cyclohexane isosorbide terephthalate)/polyvinyl alcohol. *Sci. Rep.* **2020**, *10*(1), No. 19751.

(12) Norouzi, M. R.; Ghasemi-Mobarakeh, L.; Itel, F.; Schoeller, J.; Fashandi, H.; Borzi, A.;
Neels, A.; Fortunato, G.; Rossi, R. M. Emulsion electrospinning of sodium alginate/poly (ϵ -
caprolactone) core/shell nanofibers for biomedical applications. *Nanoscale Adv.* **2022**, *4* (13),
2929–2941.

1
2
3
4 (13) Hosseini, A.; Ramezani, S.; Tabibiazar, M.; Mohammadi, M.; Golchinfar, Z.;
5
6
7 Mahmoudzadeh, M.; Jahanban-Esfahlan, A. Immobilization of α -amylase in ethylcellulose
8
9
10 electrospun fibers using emulsion-electrospinning method. *Carbohydr. Polym.* **2022**, *278*, No.
11
12
13 118919.

14
15
16
17 (14) Kurpanik, R.; Lechowska-Liszka, A.; Mastalska-Popławska, J.; Nocuń, M.; Rapacz-
18
19
20 Kmita, A.; Ścisłowska-Czarnecka, A.; Stodolak-Zych, E. Effect of ionic and non-ionic surfactant
21
22
23 on bovine serum albumin encapsulation and biological properties of emulsion-electrospun fibers.
24
25
26
27
28 *Molecules* **2022**, *27*(10), No. 3232.

29
30
31 (15) Lamarra, J.; Calienni, M. N.; Rivero, S.; Pinotti, A. Electrospun nanofibers of poly (vinyl
32
33
34 alcohol) and chitosan-based emulsions functionalized with cabreuva essential oil. *Int. J. Biol.*
35
36
37
38
39 *Macromol.* **2020**, *160*, 307–318.

40
41
42 (16) Dehghani, S.; Noshad, M.; Rastegarzadeh, S.; Hojjati, M.; Fazlara, A. Electrospun chia
43
44
45 seed mucilage/PVA encapsulated with green cardamom essential oils: Antioxidant and
46
47
48
49
50 antibacterial property. *Int. J. Biol. Macromol.* **2020**, *161*, 1–9.

- 1
2
3
4 (17) Mínguez-García, D.; Breve, N.; Capablanca, L.; Bonet-Aracil, M.; Díaz-García, P.;
5
6
7 Gisbert-Payá, J. Liquid oil trapped inside PVA electrospun microcapsules. *Polymers* **2022**, *14*
8
9
10 (23), No. 5242.
11
12
13
14 (18) Partheniadis, I.; Stathakis, G.; Tsalavouti, D.; Heinämäki, J.; Nikolakakis, I. Essential Oil–
15
16
17 Loaded Nanofibers for Pharmaceutical and Biomedical Applications: A Systematic Mini-
18
19
20 Review. *Pharmaceutics* **2022**, *14* (9), No. 1799.
21
22
23
24
25 (19) Zhang, C.; Feng, F.; Zhang, H. Emulsion electrospinning: Fundamentals, food
26
27
28 applications and prospects. *Trends Food Sci Technol* **2018**, *80*, 175–186.
29
30
31
32
33 (20) Tavassoli-Kafrani, E.; Goli, S. A. H.; Fathi, M. Encapsulation of orange essential oil using
34
35
36 cross-linked electrospun gelatin nanofibers. *Food Bioprocess Technol.* **2018**, *11*, 427–434.
37
38
39
40 (21) Ansarifard, E.; Moradinezhad, F. Encapsulation of thyme essential oil using electrospun
41
42
43 zein fiber for strawberry preservation. *Chem. Biol. Technol. Agric* **2022**, *9*, 2–11.
44
45
46
47
48 (22) Ebadi Ghareh Koureh, L.; Ganjloo, A.; Hamishehkar, H.; Bimakr, M. Fabrication and
49
50
51 characterization of costmary essential oil loaded salep-polyvinyl alcohol fast-dissolving
52
53
54 electrospun nanofibrous mats. *J. Food Meas. Charact.* **2023**, *17*, 3076–3093.
55
56
57
58
59
60

1
2
3
4 (23) Kesici Güler, H.; Cengiz Çallıoğlu, F.; Sesli Çetin, E. Antibacterial PVP/cinnamon
5
6
7 essential oil nanofibers by emulsion electrospinning. *J. Text. Inst.* **2019**, *110*(2), 302–310.
8
9

10
11 (24) Ghasemi, M.; Miri, M. A.; Najafi, M. A.; Tavakoli, M.; Hadadi, T. Encapsulation of
12
13
14 Cumin essential oil in zeinelectrospun fibers: Characterization and antibacterial effect. *J. Food*
15
16
17 *Meas. Charact.* **2022**, *16*(2), 1613–1624.
18
19

20
21
22 (25) de Souza, E. J. D.; Kringel, D. H.; Dias, A. R. G.; da Rosa Zavareze, E. Polysaccharides
23
24
25 as wall material for the encapsulation of essential oils by electrospun technique. *Carbohydr.*
26
27
28 *Polym.* **2021**, *265*, No. 118068.
29
30

31
32
33 (26) Meena, N. K.; Meena, R. S.; Singh, R.; Verma, A. K.; Choudhary, S.; Singh, B.; Meena,
34
35
36 A. D.; Ravi, Y.; Meena, M. Managed pollination is a much better way of increasing productivity
37
38
39 and essential oil content of dill seeds crop. *Sci. Rep.* **2022**, *12*(1), No. 13134.
40
41
42

43
44 (27) Kaur, V.; Kaur, R.; Bhardwaj, U. A review on dill essential oil and its chief compounds as
45
46
47 natural biocide. *Flavour Fragr. J.* **2021**, *36*(3), 412–431.
48
49
50
51
52
53
54
55
56
57
58
59
60

1
2
3
4 (28) Sharma, R.; Salwan, R.; Sharma, M.; Sharma, A.; Sharma, V. Biochemical
5
6
7 characterization of volatile compounds and antimicrobial activity of *Anethum graveolens* seeds.
8

9
10 *Vegetos* **2023**, <https://doi.org/10.1007/s42535-023-00641-1>
11
12

13
14 (29) Liu, T. T.; Gou, L. J.; Zeng, H.; Zhou, G.; Dong, W. R.; Cui, Y.; Cai, Q.; Chen, Y. X.
15
16
17 Inhibitory Effect and Mechanism of Dill Seed Essential Oil on *Neofusicoccum parvum* in
18
19
20 Chinese Chestnut. *Separations* **2022**, *9*(10), No. 296.
21
22

23
24
25 (30) Sipango, N.; Ravhuhali, K. E.; Sebola, N. A.; Hawu, O.; Mabelebele, M.; Mokoboki, H.
26
27
28 K.; Moyo, B. Prickly Pear (*Opuntia spp.*) as an Invasive Species and a Potential Fodder Resource
29
30
31 for Ruminant Animals. *Sustainability* **2022**, *14*(7), No. 3719.
32
33

34
35
36 (31) Mannai, F.; Elhleli, H.; Dufresne, A.; Elaloui, E.; Moussaoui, Y. *Opuntia* (cactaceae)
37
38
39 fibrous network-reinforced composites: thermal, viscoelastic, interfacial adhesion and
40
41
42 biodegradation behavior. *Fibers Polym.* **2020**, *21*, 2353–2363.
43
44

45
46
47 (32) Mannai, F.; Elhleli, H.; Ammar, M.; Passas, R.; Elaloui, E.; Moussaoui, Y. Green process
48
49
50 for fibrous networks extraction from *Opuntia* (Cactaceae): Morphological design, thermal and
51
52
53 mechanical studies. *Ind. Crops Prod.* **2018**, *126*, 347–356.
54
55

1
2
3
4 (33) Mannai, F.; Ammar, M.; Yanez, J. G.; Elaloui, E.; Moussaoui, Y. Cellulose fiber from
5
6
7 Tunisian Barbary Fig “*Opuntia ficus-indica*” for papermaking. *Cellulose* **2016**, *23*, 2061–2072.

8
9
10
11 (34) Mannai, F.; Ammar, M.; Yanez, J. G.; Elaloui, E.; Moussaoui, Y. Alkaline delignification
12
13
14 of cactus fibres for pulp and papermaking applications. *J. Polym. Environ.* **2018**, *26*, 798–806.

15
16
17
18 (35) Elhleli, H.; Mannai, F.; ben Mosbah, M.; Khiari, R.; Moussaoui, Y. Biocarbon Derived
19
20
21 from *Opuntia ficus indica* for p-Nitrophenol Retention. *Processes* **2020**, *8*(10), No. 1242.

22
23
24
25
26 (36) Mannai, F.; Elhleli, H.; Yılmaz, M.; Khiari, R.; Belgacem, M.N.; Moussaoui, Y.
27
28
29 Precipitation solvents effect on the extraction of mucilaginous polysaccharides from *Opuntia*
30
31
32 *ficus-indica* (Cactaceae): Structural, functional and rheological properties. *Ind. Crops Prod.*
33
34
35 **2023**, *202*, No. 117072.

36
37
38
39
40 (37) Tosif, M. M.; Najda, A.; Bains, A.; Kaushik, R.; Dhull, S. B.; Chawla, P.; Walasek-
41
42
43 Janusz, M. A comprehensive review on plant-derived mucilage: Characterization, functional
44
45
46 properties, applications, and its utilization for nanocarrier fabrication. *Polymers* **2021**, *13*(7), No.
47
48
49
50 1066.

1
2
3
4 (38) Otálora, M. C.; Wilches-Torres, A.; Gómez Castaño, J. A. Spray-Drying
5
6
7 Microencapsulation of Pink Guava (*Psidium guajava*) Carotenoids Using Mucilage from *Opuntia*
8
9
10 *ficus-indica* Cladodes and *Aloe Vera* Leaves as Encapsulating Materials. *Polymers* **2022**, *14* (2),
11
12
13 No. 310.

14
15
16
17 (39) Camelo Caballero, L. R.; Wilches-Torres, A.; Cárdenas-Chaparro, A.; Gómez Castaño, J.
18
19
20 A.; Otálora, M. C. Preparation and physicochemical characterization of softgels cross-linked with
21
22
23 cactus mucilage extracted from cladodes of *Opuntia Ficus-Indica*. *Molecules* **2019**, *24*(14), No.
24
25
26
27 2531.

28
29
30
31 (40) Gheribi, R.; Puchot, L.; Verge, P.; Jaoued-Grayaa, N.; Mezni, M.; Habibi, Y.; Khwaldia,
32
33
34 K. Development of plasticized edible films from *Opuntia ficus-indica* mucilage: A comparative
35
36
37
38 study of various polyol plasticizers. *Carbohydr. Polym.* **2018**, *190*, 204–211.

39
40
41
42 (41) Yang, H.; Wen, P.; Feng, K.; Zong, M. H.; Lou, W. Y.; Wu, H. Encapsulation of fish oil
43
44
45
46 in a coaxial electrospun nanofibrous mat and its properties. *RSC Adv.* **2017**, *7* (24), 14939–
47
48
49 14946.

1
2
3
4 (42) García-Moreno, P. J.; Stephansen, K.; van der Kruijs, J.; Guadix, A.; Guadix, E. M.;
5
6
7 Chronakis, I. S.; Jacobsen, C. Encapsulation of fish oil in nanofibers by emulsion
8
9
10 electrospinning: Physical characterization and oxidative stability. *J. Food Eng.* **2016**, *183*, 39–49.
11
12

13
14 (43) Gómez-Mascaraque, L. G.; Lagarón, J. M.; López-Rubio, A. Electrospayed gelatin
15
16
17 submicroparticles as edible carriers for the encapsulation of polyphenols of interest in functional
18
19
20
21 foods. *Food Hydrocolloids* **2015**, *49*, 42–52.
22
23

24
25 (44) Noumi, E.; Ahmad, I.; Adnan, M.; Merghni, A.; Patel, H.; Haddaji, N.; Nouha Bouali, N.;
26
27
28 Alabbosh, K. F.; Ghannay, S.; Aouadi, K.; Kadri, K.; Polito, F.; Snoussi, M.; De Feo, V. GC/MS
29
30
31
32 profiling, antibacterial, anti-quorum sensing, and antibiofilm properties of *Anethum graveolens*
33
34
35 L. essential oil: molecular docking study and in-silico ADME profiling. *Plants* **2023**, *12* (10),
36
37
38
39 No. 1997.
40
41

42
43 (45) Ma, B.; Ban, X.; Huang, B.; He, J.; Tian, J.; Zeng, H.; Chen, Y.; Wang, Y. Interference
44
45
46 and mechanism of dill seed essential oil and contribution of carvone and limonene in preventing
47
48
49
50 Sclerotinia rot of rapeseed. *PloS One* **2015**, *10* (7), No. e0131733.
51
52
53
54
55
56
57
58
59
60

1
2
3
4 (46) Li, H.; Zhou, W.; Hu, Y.; Mo, H.; Wang, J.; Hu, L. GC-MS analysis of essential oil from
5
6
7 *Anethum graveolens* L (dill) seeds extracted by supercritical carbon dioxide. *Trop. J. Pharm.*
8
9
10 *Res.* **2019**, *18* (6), 1291–1296.

11
12
13
14 (47) Rafiq, M.; Hussain, T.; Abid, S.; Nazir, A.; Masood, R. J. M. R. E. Development of
15
16
17 sodium alginate/PVA antibacterial nanofibers by the incorporation of essential oils. *Mater. Res.*
18
19
20
21 *Express* **2018**, *5* (3), No. 035007.

22
23
24
25 (48) Çallıoğlu, F. C.; Güler, H. K.; Çetin, E. S. Emulsion electrospinning of bicomponent poly
26
27
28 (vinyl pyrrolidone)/gelatin nanofibers with thyme essential oil. *Mater. Res. Express* **2019**, *6* (12),
29
30
31
32 No. 125013.

33
34
35
36 (49) Kurd, F.; Fathi, M.; Shekarchizadeh, H. Basil seed mucilage as a new source for
37
38
39 electrospinning: Production and physicochemical characterization. *Int. J. Biol. Macromol.* **2017**,
40
41
42
43 *95*, 689–695.

44
45
46
47 (50) Wen, P.; Zhu, D. H.; Wu, H.; Zong, M. H.; Jing, Y. R.; Han, S. Y. Encapsulation of
48
49
50 cinnamon essential oil in electrospun nanofibrous film for active food packaging. *Food Control*
51
52
53
54 **2016**, *59*, 366–376.

1
2
3
4 (51) Krumreich, F. D.; Prietsch, L. P.; Antunes, M. D.; Jansen-Alves, C.; Mendonça, C. R. B.,
5
6
7 Borges, C. D.; Zavareze, E. D. R.; Zambiasi, R. C. Avocado oil incorporated in ultrafine zein
8
9
10 fibers by electrospinning. *Food Biophys.* **2019**, *14*, 383–392.

11
12
13
14 (52) Ura, D. P.; Karbowniczek, J. E.; Szewczyk, P. K.; Metwally, S.; Kopyściański, M.;
15
16
17 Stachewicz, U. Cell integration with electrospun PMMA nanofibers, microfibers, ribbons, and
18
19
20 films: a microscopy study. *Bioengineering* *6*(2), No. 41.

21
22
23
24 (53) Rezaeinia, H.; Emadzadeh, B.; Ghorani, B. Electrospun balangu (*Lallemantia royleana*)
25
26
27 hydrocolloid nanofiber mat as a fast-dissolving carrier for bergamot essential oil. *Food*
28
29
30
31
32 *Hydrocolloids* **2020**, *100*, No. 105312.

33
34
35
36 (54) de Oliveira, E. R. M.; Vieira, R. P. Synthesis and characterization of poly (limonene) by
37
38
39 photoinduced controlled radical polymerization. *J. Polym. Environ.* **2020**, *28*, 2931–2938.

40
41
42
43 (55) Sanei-Dehkordi, A.; Moemenbellah-Fard, M. D.; Saffari, M.; Zarenezhad, E.; Osanloo, M.
44
45
46 Nanoliposomes containing limonene and limonene-rich essential oils as novel larvicides against
47
48
49 malaria and filariasis mosquito vectors. *BMC Complementary Med. Ther.* **2022**, *22*(1), No. 140.

1
2
3
4 (56) Carvalho, R. A.; de Oliveira, A. C. S.; Santos, T. A.; Dias, M. V.; Yoshida, M. I.; Borges,
5
6
7 S. V. WPI and cellulose nanofibres bio-nanocomposites: effect of thyme essential oil on the
8
9
10 morphological, mechanical, barrier and optical properties. *J. Polym. Environ.* **2020**, *28*, 231–
11
12
13 241.

14
15
16
17 (57) Elhleli, H.; Mannai, F.; Khiari, R.; Moussaoui, Y. The use of mucilage extracted from
18
19
20
21 *Opuntia ficus indica* as microencapsulating shell. *J. Serb. Chem. Soc.* **2021**, *86*(1), 25–38.
22
23

24
25 (58) Contreras-Padilla, M.; Rodríguez-García, M. E.; Gutiérrez-Cortez, E.; del Carmen
26
27
28 Valderrama-Bravo, M.; Rojas-Molina, J. I.; Rivera-Muñoz, E. M. Physicochemical and
29
30
31 rheological characterization of *Opuntia ficus* mucilage at three different maturity stages of
32
33
34 cladode. *Eur. Polym. J.* **2016**, *78*, 226–234.
35
36
37

38
39 (59) Vargas-Solano, S. V.; Rodríguez-González, F.; Martínez-Velarde, R.; Morales-García, S.
40
41
42 S.; Jonathan, M. P. Removal of heavy metals present in water from the Yautepec River Morelos
43
44
45 México, using *Opuntia ficus-indica* mucilage. *Environ. Adv.* **2022**, *7*, No. 100160.
46
47
48

49
50 (60) García-Barradas, O.; Esteban-Cortina, A.; Mendoza-Lopez, M. R.; Ortiz-Basurto, R. I.;
51
52
53 Díaz-Ramos, D. I.; Jiménez-Fernández, M. Chemical modification of *Opuntia ficus-indica*
54
55
56

1
2
3 mucilage: characterization, physicochemical, and functional properties. *Polym. Bull.* **2022**, *80*,
4
5
6
7 8783–8798.

8
9
10
11 (61) Fahami, A.; Fathi, M. Development of cress seed mucilage/PVA nanofibers as a novel
12
13
14 carrier for vitamin A delivery. *Food Hydrocolloids.* **2018**, *81*, 31–38.

15
16
17
18 (62) Urena-Saborio, H.; Alfaro-Viquez, E.; Esquivel-Alvarado, D.; Madrigal-Carballo, S.;
19
20
21
22 Gunasekaran, S. Electrospun plant mucilage nanofibers as biocompatible scaffolds for cell
23
24
25 proliferation. *Int. J. Biol. Macromol.* **2018**, *115*, 1218–1224.

26
27
28
29 (63) Madera-Santana, T. J.; Vargas-Rodríguez, L.; Núñez-Colín, C. A.; González-García, G.;
30
31
32
33 Peña-Caballero, V.; Núñez-Gastélum, J. A.; Gallegos-Vázquez, C.; Rodríguez-Núñez, J. R.
34
35
36 Mucilage from cladodes of *Opuntia spinulifera* Salm-Dyck: chemical, morphological, structural
37
38
39 and thermal characterization. *CYTA J Food* **2018**, *16*(1), 650–657.

40
41
42
43 (64) Gheybi, N.; Pirouzifard, M. K.; Almasi, H. *Ornithogalum cuspidatum* mucilage as a new
44
45
46
47 source of plant-based polysaccharide: Physicochemical and rheological characterization. *J. Food*
48
49
50 *Meas. Charact.* **2021**, *15*, 2184–2201.

1
2
3
4 (65) Jing, F. Y.; Zhang, Y. Q. Unidirectional nanopore dehydration induces an anisotropic
5
6
7 polyvinyl alcohol hydrogel membrane with enhanced mechanical properties. *Gels* **2022**, *8* (12),
8
9
10 No. 803.

11
12
13
14 (66) Hadad, S.; Goli, S. A. H. Fabrication and characterization of electrospun nanofibers using
15
16
17 flaxseed (*Linum usitatissimum*) mucilage. *Int. J. Biol. Macromol.* **2018**, *114*, 408–414.

18
19
20
21
22 (67) Kurusu, R. S.; Demarquette, N. R. Surface modification to control the water wettability of
23
24
25 electrospun mats. *Int. Mater. Rev.* **2019**, *64* (5), 249–287.

26
27
28
29 (68) Biduski, B.; Kringel, D. H.; Colussi, R.; dos Santos Hackbart, H. C.; Lim, L. T.; Dias, A.
30
31
32 R. G.; da Rosa Zavareze, E. Electrospayed octenyl succinic anhydride starch capsules for
33
34
35 rosemary essential oil encapsulation. *Int. J. Biol. Macromol.* **2019**, *132*, 300–307.

36
37
38
39 (69) Estevez-Areco, S.; Guz, L.; Candal, R.; Goyanes, S. Release kinetics of rosemary
40
41
42 (Rosmarinus officinalis) polyphenols from polyvinyl alcohol (PVA) electrospun nanofibers in
43
44
45 several food simulants. *Food Packag. Shelf Life* **2018**, *18*, 42–50.

46
47
48
49 (70) Wongkanya, R.; Teeranachaideekul, V.; Makarasen, A.; Chuysinuan, P.; Yingyuad, P.;
50
51
52 Nooeaid, P.; Techasakul, S.; Chuenchom, L.; Dechtrirat, D. Electrospun poly (lactic acid)
53
54
55

1
2
3
4 nanofiber mats for controlled transdermal delivery of essential oil from *Zingiber cassumunar*
5
6
7 Roxb. *Mater. Res. Express* **2020**, *7*(5), No. 055305.

8
9
10 (71) Mohajeri, P.; Hematian Sourki, A.; Mehregan Nikoo, A.; Ertas, Y. N. Fabrication,
11
12 characterisation and antimicrobial activity of electrospun *Plantago psyllium* L. seed gum/gelatine
13
14 nanofibres incorporated with *Cuminum cyminum* essential oil nanoemulsion. *Int. J. Food Sci.*
15
16
17
18
19
20
21 *Technol.* *58*(4), 1832-1840.

22
23
24 (72) Lan, W.; Wang, S.; Chen, M.; Sameen, D. E.; Lee, K.; Liu, Y. Developing poly (vinyl
25
26 alcohol)/chitosan films incorporate with d-limonene: Study of structural, antibacterial, and fruit
27
28
29
30
31
32 preservation properties. *Int. J. Biol. Macromol.* **2020**, *145*, 722–732.

33
34
35 (73) Kumar, N.; Khurana, S. M.; Pandey, V. N. Application of clove and dill oils as an
36
37
38
39
40
41
42 alternative of salphos for chickpea food seed storage. *Sci. Rep.* **2021**, *11* (1), No. 10390.

43
44 (74) Teneva, D.; Denkova, Z.; Denkova-Kostova, R.; Goranov, B.; Kostov, G.; Slavchev, A.;
45
46
47 Hristiva-Ivanova, Y.; Uzunova, G.; Degraeve, P. Biological preservation of mayonnaise with
48
49
50
51
52
53
54
55
56
57
58
59
60 Lactobacillus plantarum LBRZ12, dill, and basil essential oils. *Food Chem.* **2021**, *344*, No.
128707.